GEOLOGICA CARPATHICA, FEBRUARY 2021, 72, 1, 26–47 https://doi.org/10.31577/GeolCarp.72.1.3

A Lower Miocene pyroclastic-fall deposit from the Bükk Foreland Volcanic Area, Northern Hungary: Clues for an eastward-located source

MÁTYÁS HENCZ[1,✉], TAMÁS BIRÓ[1], ZOLTÁN CSERI[1], DÁVID KARÁTSON[1], EMŐ MÁRTON[2], KÁROLY NÉMETH[3], ALEXANDRU SZAKÁCS[4], ZOLTÁN PÉCSKAY[5] and ISTVÁN JÁNOS KOVÁCS[6]

[1]Eötvös University, Faculty of Science, Department of Physical Geography, Pázmány Péter sétány 1/C, H-1117 Budapest, Hungary; ✉hemuabt@caesar.elte.hu
[2]Mining and Geological Survey of Hungary, Paleomagnetic Laboratory, Homonna str. 9., H-1118 Budapest, Hungary
[3]Massey University, School of Agriculture and Environment, Private Bag 11 222 Palmerston North, 4442 New Zealand
[4]Romanian Academy, Institute of Geodynamics, Department of Endogene Processes, Natural Hazard and Risk, 19-21 Jean-Louis Calderon St., R-020032 Bucharest-37, Romania
[5]Institute of Nuclear Research (ATOMKI), Isotope Climatology and Environmental Research Centre (ICER); K–Ar Group, Bem tér 18/c, H-4026 Debrecen, Hungary
[6]Hungarian Academy of Science, Research Center for Astronomy and Earth Sciences, Lendület Pannon LitH2Oscope Research Group, Csatkai Endre u. 6-8, H-9400 Sopron, Hungary

(Manuscript received June 27, 2020; accepted in revised form January 4, 2021; Associate Editor: Lukáš Krmíček)

Abstract: Detailed investigation of a Lower Miocene Plinian pyroclastic sequence that crops out in the Bükk Foreland Volcanic Area (BFVA) in Northern Hungary is presented here. The studied eruptive products are part of a ca. 50 metres thick pyroclastic succession comprising of a basal ignimbrite that is covered by stratified pyroclastic unit including a topmost ignimbrite (Mangó ignimbrite unit, part of the Lower Pyroclastic Complex). The investigated pyroclastic unit is part of the Mangó ignimbrite unit, and consists of a pyroclastic fallout deposit, a ground-surge deposit, and an ignimbrite, all indicating a complete Plinian eruption phase. This pyroclastic succession has been identified in three locations, which crops out along a ~20 km long, SW–NE transect in the BFVA (two in the western, and one in the eastern part). The pyroclastic rocks in these sites are correlated well on the basis of the lithologically and texturally similar layers and their identical field volcanological properties. The correlation is also supported by the paleomagnetic signature of the two ignimbrites (upper ignimbrite – declination: 275–302°, lower ignimbrite with overprint magnetization – declination: 320–334°). The paleomagnetic directions of the stratigraphically upper ignimbrite suggest that this sequence belongs to the oldest known pyroclastic rock assemblages of the BFVA (Lower Pyroclastic Complex, deposited between 18.5 and 21 Ma according to previously published K/Ar dating results in good agreement with paleomagnetic measurements). Based on proximal-to-distal variations in the grain size of the pyroclastic fallout deposit (with maximal thickness is 71 cm), a potential source region to the east (or northeast, or southeast) of the BFVA has been inferred in a relatively close distance (~5–15 km). The (north)eastward-located source region is also supported by comparison of the characteristics of the studied fallout deposit with the spatial distribution of selected Plinian fallout tephra from worldwide examples using their digitalized isopach maps.

Keywords: Plinian, ignimbrites, volcano stratigraphy, paleomagnetism, pyroclastic fall, granulometry, source region.

Introduction

Large-scale silicic explosive volcanism occurred during Early to Middle Miocene times in the vicinity of the Bükk Foreland Volcanic Area (BFVA) in Northern Hungary (Fig. 1, Schréter 1939; Pantó 1961; Pantó 1962; Szakács et al. 1998; Lukács et al. 2018). Miocene primary volcaniclastic rocks are well-exposed in widely distributed outcrops (mostly abandoned quarries and wine cellars). The volcaniclastic succession is also known from boreholes (usually buried beneath younger sediments throughout the Pannonian Basin, or adjacent, mostly coeval sedimentary basins: e.g. Transylvanian Basin, Vienna Basin; Fig. 1) (Szakács et al. 2012; Lukács et al. 2018; Rybár et al. 2019). The pyroclastic units of the volcaniclastic piles consist mostly of number of a 2–30 m thick pumice-bearing pyroclastic density current deposits, i.e. ignimbrites (Schréter 1939; Pantó 1962; Capaccioni et al. 1995; Szakács et al. 1998; Lukács et al. 2018; Biró et al. 2020). The ignimbrites are separated from each other by pyroclastic fallout deposits, reworked volcaniclastics and paleosols (Capaccioni et al. 1995; Szakács et al. 1998; Biró et al. 2020).

Correlating specific volcaniclastic units from one outcrop to the next is a real challenge in the BFVA due to the general weathered appearance of the deposits, the scarcity of the exposures suitable for analysis, and their mosaic-like and isolated occurrence (Capaccioni et al. 1995; Szakács et al. 1998).

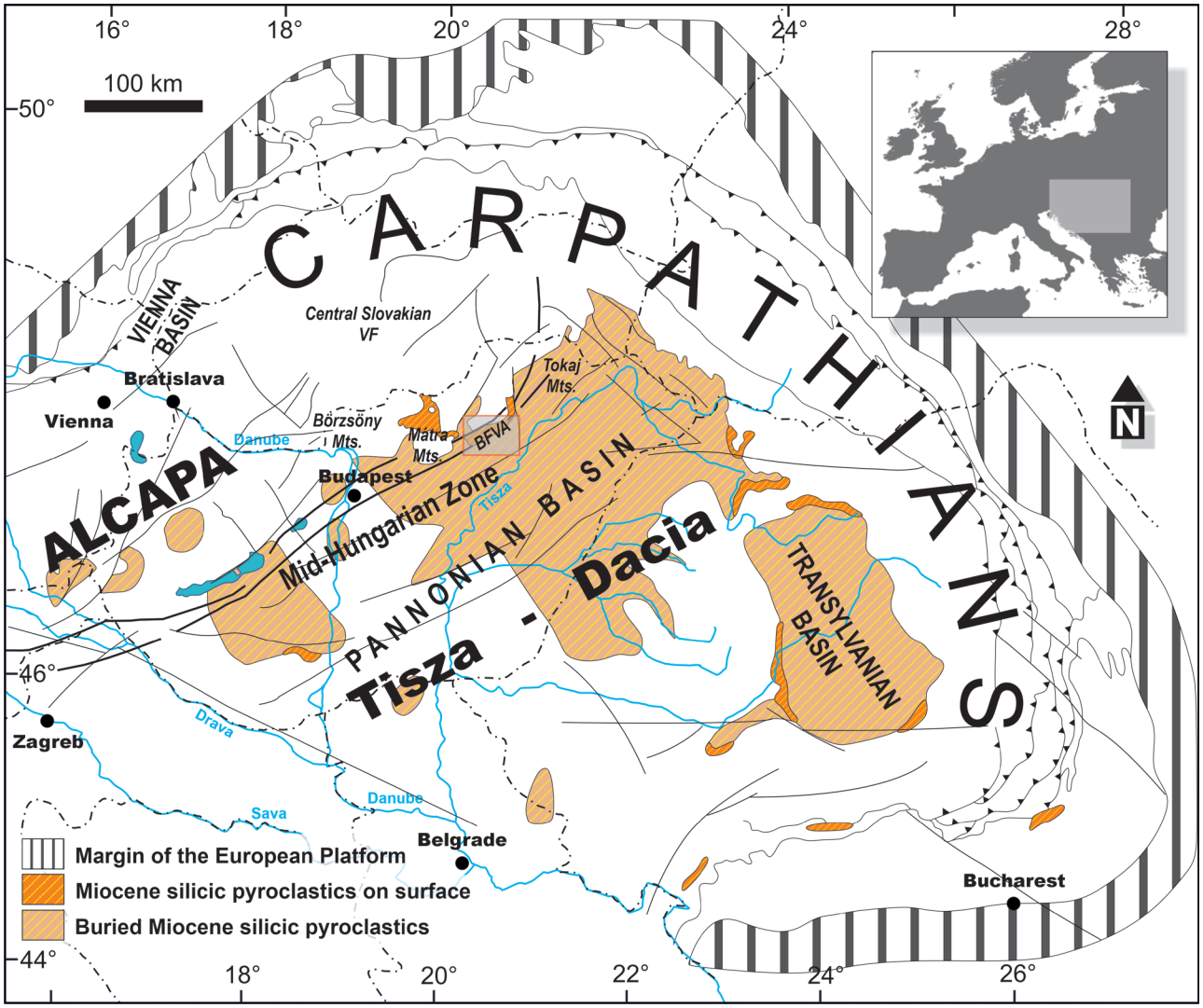

Fig. 1. Distribution of Miocene felsic pyroclastic rocks within the Pannonian Basin (Central Europe). The map was modified after Pécskay et al. (2006) and Szakács et al. (2018). Buried pyroclastics exposed by drillings.

A number of studies have been performed so far, which clarified the stratigraphical position of a single or a few units of the formations using various investigation methods, most importantly, field-based volcanic stratigraphy (Capaccioni et al. 1995; Szakács et al. 1998; Biró et al. 2020), paleomagnetic studies (Márton & Pécskay 1998; Márton et al. 2007) or geochemical comparison (Harangi et al. 2005; Lukács et al. 2015). In this paper we use the term "pyroclastic complex" for the large units of the vertical stratigraphical column, which can be distinguished from each other based on chronostratigraphic, magnetostratigraphic, or chemostratigraphic features as used elsewhere (e.g. Martí et al. 2018; Németh & Palmer 2019). The pyroclastic complexes can be divided into several 2nd order subunits (e.g. members; Biró et al. 2020) showing identical field appearance (e.g. bedded fine tuff) at specific field locations. In turn, the subunits can be subdivided into deposits from several eruption (or inter-eruptive) events (e.g. formation of soils) based on field observations, petrographical properties and granulometry (Martí et al. 2018; Németh & Palmer 2019).

Several volcanological studies already emphasized the importance of the pyroclastic fallout horizons as eruption events associated with major ignimbrite-forming eruptions from a field correlational point of view especially in poorly exposed volcanic terrains (Hildreth & Mahood 1985; Wilson 1993; Bonadonna et al. 1998; Coltelli et al. 2000; Wilson 2001; Martí et al. 2018; Németh & Palmer 2019). Fall deposits, which can be found directly under an ignimbrite, are commonly associated with the initial phase of major ignimbrite events and can be used for locating source regions (Marti et al. 2016; Edgar et al. 2017; Buckland et al. 2020). The spatial distribution of thickness and grain-size characteristics (average and maximal diameter of the largest lithic and pumice clasts) of the volcaniclastic units as well as features indicating pyroclast transport direction (if available) may be used as vectors of the relative location of the eruption centre(s), e.g.

increasing grain size of lithics or pumice (Eychenne et al. 2012; Edgar et al. 2017; Mele et al. 2020), axis of asymmetric bomb sags (Arce et al. 2003) or the direction inferred from the anisotropy of magnetic susceptibility (AMS) signal of the volcanic deposit (Cagnoli & Tarling 1997; Ort et al. 2015; Kischer et al. 2020). An earlier study already attempted to locate at least one eruption centre around the BFVA using the general granulometric properties of fallout horizons mapped out and some lateral transport direction indicators identified in various exposures (Szakács et al. 1998); however, as far as we know these horizons do not represent the same eruptive units, thus they cannot be correlated convincingly.

Here, we present the results of the volcanological investigation of a Plinian succession of the Lower Pyroclastic Complex cropping out in three distinct sites of the BFVA (Fig. 2). Their correlation was established by using a combination of paleomagnetic methods and physical volcanological field observations, such as stratigraphic considerations and thickness measurement of the fallout layer. The latter was complemented with the determination of the main granulometric features. Using physical volcanological constraints, it is possible to infer the direction of the source region of a pyroclastic fall deposit (e.g. Marti et al. 2016; Edgar et al. 2017; Buckland et al. 2020), which, as mentioned above, is often associated with the initial phase of an ignimbrite-forming eruption (Sparks et al. 1973; Wilson 1993; Fierstein & Hildreth 1992; Druitt 1998; Vespa et al. 2006). Thus, in this work the source region of the coeval, overlying ignimbrite is considered as the source of the fall deposit, too. Our approach can be considered as a gap-filling work in the BFVA in terms of event-scale geological mapping which makes it possible to obtain information about one single eruption, and the respective eruption centre.

Geological background

During the Early to Middle Miocene silicic volcanism in the Carpatho-Pannonian Region, voluminous pyroclastic and other volcaniclastic deposits were emplaced in Northern Hungary. Today, these mostly indurated, partly uncemented formations crop out in isolated but numerous spots on a large area of the Carpatho-Pannonian Region spanning from the Börzsöny and Mátra Mountains in the west, throughout the BFVA, to the Eperjes-Tokaj Mountains (Slanské vrchy lub Zemplínské vrchy in Slovakia) in the east (Fig. 1, Pantó 1962; Hámor et al.1978; Szabó et al. 1992; Szakács et al. 1998;

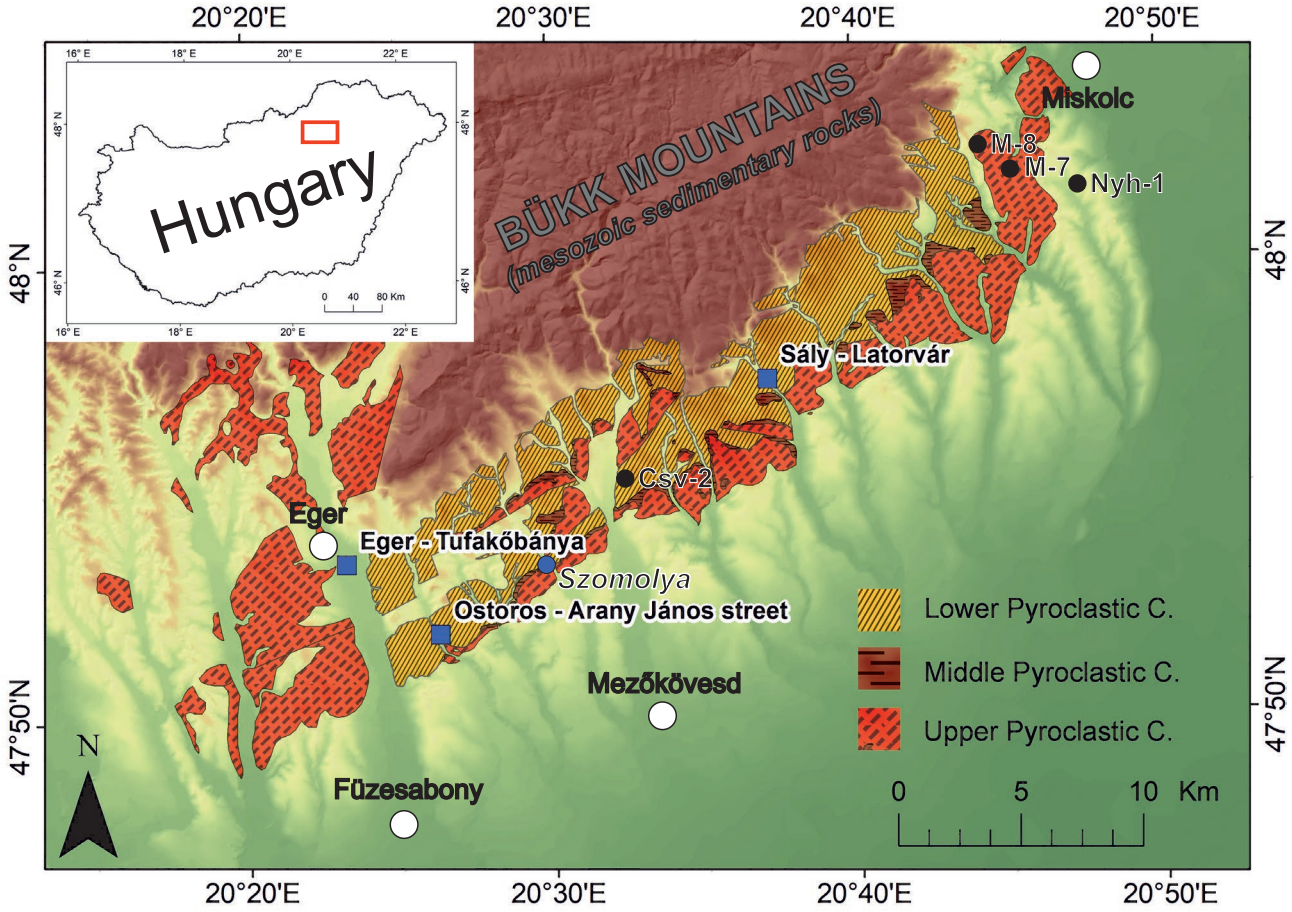

Fig. 2. Volcanological map of the Bükk Foreland Volcanic Area showing the three main pyroclastic complexes (based on Szakács et al. 1998) and the outcrops investigated within this study. The most important drillings are presented with black dots.

2018; Lukács et al. 2018). Besides these areas, large-volume silicic volcanic deposits also crop out in the Central Slovakian Volcanic Field, in the Vienna Basin and in the Transylvanian Basin (Fig. 1, Konečný et al. 1995; Szakács et al. 2012; Rybár et al. 2019). In most other areas (in particular, the Great Hungarian Plain) the Miocene pyroclastic rocks are known only from boreholes, due to thick post-volcanic sedimentary cover (Lexa et al. 2010; Lukács et al. 2010; Szakács et al. 2012, 2018; Rybár et al. 2019). The BFVA was considered as a potential source area of many Miocene volcanic ash layers cropping out in Western or Southern Europe (Lukács et al. 2018) based on formerly published ages (14–17.4 Ma, e.g. several tephra horizons in the Middle Miocene Upper Freshwater Molasse, Switzerland and South Germany (Gubler et al. 1992; Rocholl et al. 2017), 17 ash beds in the La Vedova and Monte dei Corvi sections, east-central Italy (Wotzlaw et al. 2014)).

The Miocene calc-alkaline magmatism occurring on the ALCAPA (Alpine-Carpathian-Pannonian) microplate of the Carpatho-Pannonian Region was preceded by the subduction of the Magura (or Vardar) oceanic microplate, which resulted in re-fertilization and partial melting in the lithospheric mantle (Szabó et al. 1992; Kovács & Szabó 2008). Due to the eastward movement and rotation of the ALCAPA and Tisza-Dacia microplates, significant crustal thinning took place in the ALCAPA microplate (Csontos et al. 1992; Márton & Márton 1996; Márton et al 2007). At the same time normal faults were formed in the crust of the ALCAPA microplate (Fig. 1, Csontos et al. 1992). Due to the thinning of the crust (Csontos et al. 1992), the transported, re-fertilized mantle (Szabó et al. 1992; Kovács & Szabó 2008), and the upwelling asthenosphere, partial melting occurred at the mantle-crust boundary (Seghedi et al. 2004), and the resulting melts ascended towards the surface of the permeable crust hosting the extensive normal fault system (Csontos et al. 1992). A multi-level, complex magmatic system was formed, fed by melt-containing pockets at the mantle-crust boundary, as well as inside the crust (Lukács et al. 2005, 2009; Seghedi et al. 2005). From this magmatic system calc-alkaline magmas with high silica content erupted eventually causing violent explosive volcanism (Szakács & Karátson 1997; Szakács et al. 1998; Lukács et al. 2009). The volcanic eruptions are postulated to have been originated from several centres on the basis of the recognized complexity of the pyroclastic successions of the region. In addition, a general concept emerged that the thick and regionally extensive pyroclastic successions are likely to have been associated with caldera formations (Pantó 1962; Szakács et al. 1998). Recent studies (e.g. Biró et al. 2020) confirmed the early model to explain the complex nature of the BFVA volcanism (Szakács et al. 1998) pointing out that the explosivity of the volcanism was enhanced by the presence of external water during eruptions, thus phreatomagmatic (or even Phreatoplinian) events dominated a part of the ignimbrite-forming eruptions (Biró et al. 2020). The water, required to sustain the phreatomagmatic character of the eruptions, was largely available in the environment of the volcanoes as the BFVA was located in a wet lowland setting occupied by the Paratethys over most of the area (Kováč et al. 2007, 2017; Biró et al. 2020). The BFVA today is located in an inflexion zone between the upward moving Bükk Mountains (which consist dominantly of Mesozoic Bükkfennsíki Limestone Formation) and the subsiding Great Hungarian Plain (Fig. 2).

Recent studies addressing the geodynamical background of the volcanism, the eruption styles, and the characteristics of the volcanic sediments, have suggested that the type of BFVA volcanism commonly appeared as a close analogy of the Quaternary and still active Taupo Volcanic Zone in New Zealand (Wilson 1993, 2001; Lukács et al. 2018; Biró et al. 2020).

The lifespan of the volcanism in the first comprehensive chronostratigraphy work, determined by the K/Ar method applied on whole rock and biotite samples, falls roughly between 21 and 13.5 Ma, the oldest measured age being 20.7±2.0 Ma, and the youngest 13.84±0.94 Ma (Márton & Pécskay 1998). The pyroclastic succession of the BFVA has been divided traditionally into three large volcanic formations ("tuff horizons", e.g. Noszky 1931; Schréter 1939) which rather should be considered as pyroclastic complexes (Table 1, Szakács et al. 1998; Biró et al. 2020). Based on the inferred paleomagnetic rotations and K/Ar dating, the three pyroclastic complexes are characterized by the following age ranges and rotation parameters: I) Lower Pyroclastic Complex: 21–18.5 Ma (80–90° CCW rotation); II) Middle Pyroclastic Complex: 17.5–16 Ma (30° CCW rotation); and III) Upper Pyroclastic Complex: 14.5–13.5 Ma (0–10° CW rotation), respectively (Hámor et al. 1978; Márton & Márton 1996; Márton & Pécskay 1998; Márton et al. 2007). In contrast, recent studies based on zircon U–Pb ages (Lukács et al. 2015, 2018; Harangi & Lukács 2019) dated the volcanism of the BFVA roughly between 18 and 14 Ma, the measured oldest age being 18.16±0.10 Ma, and the youngest one 14.19±0.07 Ma (Lukács et al. 2018). Lukács et al. (2018) divided the volcanism into 8 "eruption phases" or "eruption events" based on zircon U–Pb ages and zircon trace element compositions as follows (Table 1): 18.2±0.3 Ma (Csv-2 from borehole, Fig. 2), 17.5±0.3 Ma (Eger ignimbrite unit), 17.055±0.024 Ma (Mangó ignimbrite unit), 16.816±0.059 Ma (Bogács unit), 16.2±0.3 Ma (Td-J eruption), 14.880±0.014 Ma (Demjén ignimbrite unit), 14.7±0.2 Ma (Tibolddaróc unit), and 14.358±0.015 Ma (Harsány ignimbrite unit). These "eruption phases" or "events" are not necessarily represented by one single eruptive unit; Lukács et al. (2018) identified them as comprising the main ignimbrite-forming eruptions during the BFVA volcanism. These "eruption phases" are chronostratigraphical or zircon trace element-chemostratigraphical units, consisting of one or more closely packed single eruptions (Lukács et al. 2018).

The Lower Pyroclastic Complex (LPC)

In this work we focus on a Plinian sequence at the upper part of the LPC, especially on the pyroclastic fallout horizon

Table 1: Stratigraphic subdivision of the BFVA succession in different former studies. The basis of stratigraphical subdivision is presented in brackets. The investigated unit is in bold.

Márton & Pécskay 1998 (paleomagnetic rotations, K–Ar age)	**Szakács et al. 1998** (field observations and main lithological properties)	**Lukács et al. 2018** (zircon U–Pb age)
Upper Pyroclastic Complex (0°; 13.5–14.5 Ma)	*Upper Tuff Complex* (*UTC*; reworked tephra, phreatomagmatic deposits, non-welded ignimbrites)	*Harsány ignimbrite unit* (14.358±0.015 Ma) *Tibolddaróc unit* (14.7±0.2 Ma) *Demjén ignimbrite unit* (14.880±0.014 Ma)
Middle Pyroclastic Complex (30°; 16–17.5 Ma)	*Upper Middle Tuff Complex* (*UMTC*; obsidian fiamme-rich welded ignimbrites, reddish-dark grey non-welded mixed pumice-scoria ignimbrites, accretionary lapilli-bearing phreatomagmatic deposits) *Lower Middle Tuff Complex* (*LMTC*; welded red ignimbrites, phreatomagmatic deposits)	*Td-J unit* (16.2±0.3 Ma) *Bogács unit* (16.816±0.059 Ma)
***Lower Pyroclastic Complex* (80–90°; 18.5–21 Ma)**	***Upper Lower Tuff Complex* (*ULTC*; reworked tuffs, pumice fall deposits, phreatomagmatic fall deposits, non-welded ignimbrites, welded ignimbrites)** *Lower Lower Tuff Complex* (*LLTC*; non-welded ignimbrites, interbedded in red conglomerates)	***Mangó ignimbrite unit* (17.055±0.024 Ma)** *Eger ignimbrite unit* (17.5±0.3 Ma) *Csv-2 unit* (18.2±0.3 Ma)

(Capaccioni et al. 1995; Szakács et al. 1998) at the base of the main ignimbrite of the Mangó ignimbrite unit of Lukács et al. (2018). The red, welded ignimbrite of the Middle Pyroclastic Complex is a hard, indurated rock enough to be able to preserve the older pyroclastic deposits (i.e. LPC); however, exposed sections of LPC are sporadic and unevenly distributed across the region.

The LPC is the thickest felsic volcanic sequence of the BFVA reaching between 140 and 300 m (Lukács et al. 2018) in thickness, also identified in boreholes in the eastern part of the BFVA (Lukács et al. 2010). The LPC can be separated into two units (Table 1; LLTC and ULTC acc. to Szakács et al. 1998). The LLTC was emplaced directly on top of Oligocene or Lower Miocene pre-volcanic sediments (Szakács et al. 1998). The major part of the LLTC is a biotite-rich, non-welded ignimbrite dated at 19.7 Ma (Capaccioni et al. 1995; Márton & Pécskay 1998; Szakács et al. 1998). The ULTC begins with reworked tephra layers, followed by Plinian and phreatomagmatic fallout horizons (e.g. in Eger–Tufakőbánya in Fig. 2; Szakács et al. 1998). These layers are overlain by another, generally non-welded ignimbrite displaying slightly welded character in some places (Szakács et al. 1998). The K/Ar age of this unit was determined at 18.7 Ma (Márton & Pécskay 1998). Pyroclastic fallout horizons were described from several outcrops, indicating that in between, or preceding the major ignimbrite-forming eruptions, sporadic and less voluminous magmatic and phreatomagmatic eruptions were taking place (Szakács et al. 1998). Taking into account the thickness variations in the fallout horizons and the distribution of the largest pumice fragments, Szakács et al. (1998) tentatively inferred an eruption centre for the LPC located south of Eger (i.e. immediately southwest of the BFVA) (Fig. 2).

Other previous studies identified the Lower and Middle Pyroclastic Complexes, and the transition in between, from boreholes drilled near the city of Miskolc (Lukács et al. 2010). As mentioned above, the LPC was separated into three units based on zircon U–Pb dating and zircon trace elements geochemistry (Table 1; Csv-2 unit, Eger ignimbrite unit, Mangó ignimbrite unit; Lukács et al. 2018). The LPC near Miskolc is represented by a generally non-welded ignimbrite, which is slightly welded in the middle part of the unit as suggested by the presence of fiamme structures (Lukács et al. 2010). Due to the thickness distribution of the ignimbrite measured in the boreholes, and the presence of the slightly welded facies of the ignimbrite, these latter authors suggested an eastern-directed eruption centre, which could be located near Miskolc (Lukács et al. 2010).

Methods

Investigated outcrops

Three outcrops investigated in this study including: Eger – Tufakőbánya (Tuff Quarry), Ostoros – Arany János street and cellars, and Sály – Latorvár (the first words referring to village names; Fig. 2). A fourth one, at Szomolya village outcrop, was not investigated in detail due to the heavily weathered conditions of the pyroclastic deposit, however its field properties (especially the thickness of the well-sorted, clast-supported lower layer) were also considered.

Two quarries – which are inactive now – have been opened in the Tihamér part of the town of Eger for the excavation of volcanic and sedimentary rocks (Electronic Supplement 1). The Eger outcrop was named as Tufakőbánya (Tuff Quarry), Tihamérbánya (Tihamér Quarry) or Andornaktálya quarry in previous publications (e.g. Capaccioni et al. 1995; Márton & Márton 1996; Szakács et al. 1998). It consists of two parts: a larger upper yard and a smaller lower yard (Electronic Supplement 1). The horizontal distance between the two yards is ca. 200 m (Electronic Supplement 1) and they represent together a more than 100 m-thick nearly continuous,

accessible pile of pyroclastic rocks. The succession of the volcanic rocks exposed in the Tufakőbánya was investigated using several methods: paleomagnetic (Márton & Márton 1996), geochemical (Póka et al. 1998; Biró et al. 2017), geochronological (Lukács et al. 2018) and field volcanological (Capaccioni et al. 1995; Szakács et al. 1998). These studies focused on the two thick pumice-bearing, poorly sorted lapilli tuffs exposed in both quarry yards, and they also referred to the diversity of the volcaniclastic sediments found in between them (as seen in the stratigraphical column in Capaccioni et al. 1995).

At the southeastern part of Ostoros village (Electronic Supplement 2) there are many wine cellars and cave houses carved in the uncemented, but stable pyroclastic rocks. Pyroclastic rocks cropping out in the Arany János street (Electronic Supplement 2), and in the cellars located above it (Gárdonyi Géza street) were investigated.

To the north of Sály village, next to the road to Latorpuszta (Electronic Supplement 3), there is a local topographic high, a small hill named Latorvár (highest point is at 279 m a.s.l., Electronic Supplement 3). At this site a welded ignimbrite outcrop was described previously (Szakács et al. 1998), classified as belonging to the Middle Pyroclastic Complex. Also, in the same publication an andesitic tuff horizon was mentioned right below the welded ignimbrite. Here, this hillside outcrop was re-investigated in detail.

Granulometric and paleomagnetic methods

The direction of the source region was inferred based on the granulometric and field properties of a prominent pyroclastic fallout layer found right below the ULTC (acc. to Szakács et al. 1998) or Mangó ignimbrite unit (acc. to Lukács et al. 2018). Other "traditional" tephra dispersal models and methods (e.g. Walker 1971; Wilson 1993; Bonadonna et al. 1998; Pyle et al. 2006; Alfano et al. 2016; Janebo et al. 2016; Pedrazzi et al. 2019) cannot be used here, because the scarcity of reliable locations prevents to collect a sufficient amount of reliable thickness data from the same tephra unit across the region. Only the above-mentioned three outcrops could be used reliably so far complemented with the Szomolya outcrop.

The granulometric measurements were carried out at the Department of Physical Geography of the Eötvös Loránd University, Budapest, Hungary. Sieving was not feasible due to the cemented and altered condition of the samples. Instead, we concentrated on other relevant granulometric features of the deposit: after hand-crushing the samples, the lithoclasts and quartz phenocrysts were separated, and their largest diameter was measured, respectively (following Simmons et al. 2017 and Mele et al. 2020). These rock components were not affected by the intense weathering, and they are also hard enough to resist the hand-crushing procedure. The average diameter five and ten largest lithic clasts and quartz phenocrysts, respectively, were measured (e.g. Simmons et al. 2017).

Paleomagnetic investigations were carried out on 45 field-oriented samples collected from four sites (including both Mangó and Eger ignimbrite units, acc. to Table 1) in order to support the correlation of the pyroclastic units. Pumice and matrix samples were drilled in the field using a low-voltage electric drilling machine. In the Paleomagnetic Laboratory of the Mining and Geological Survey of Hungary the natural remanent magnetization (NRM) of the samples were measured with JR-4 and JR5A spinner magnetometers, and the low-field magnetic susceptibility with a KLY-2 Kappabridge instrument. Alternating field (AF) and more often thermal demagnetization technique was used in several steps in order to reveal the whole spectrum of the possibly present components of the NRM, which may have been imprinted during the cooling of the rocks (primary NRM) or any time after. In case of thermal demagnetization, the susceptibility was re-measured after each heating step in order to monitor the possible changes in the magnetic mineralogy. The demagnetization was made in a large number of steps on pilot samples from each sampling site (in case of thermal method starting from 150 °C up to 500 °C in 50 °C steps, and, over this temperature in 25 °C steps up to 575 °C). Based on the demagnetization behaviour of the pilot samples, others were demagnetized in fewer steps. On the welded pyroclastic rock samples mostly alternating field demagnetization was applied. Determination of the paleomagnetic direction for each sample was based on the results of principal component analysis (Kirschvink 1980). The site-mean paleomagnetic directions with statistical parameters were computed using the method of Fisher (1953).

Results

Field observations

In Eger, in the lower quarry yard of the Tufakőbánya, a 30 m-thick, massive, poorly-sorted, large pumice- and lithic-bearing lapilli tuff crops out (Figs. 3, 4c). The base and thus the direct lower contact of this lapilli tuff is not exposed. On the top of the massive lapilli tuff there is a 2 m-thick stratified succession of volcaniclastic deposits, including well-sorted layers and, in some parts, cross-bedded layers. These layers consist of fine-grained tuff and coarse-grained lapilli tuff. The succession above this unit is not visible in this quarry yard. In the upper quarry yard the outcrop begins with a complex succession comprising pumice- and lithic-bearing reworked volcaniclastic deposits and several well-sorted lapilli tuffs or cross-bedded tuffs with accretionary lapilli, and poorly-sorted, pumice-bearing lapilli tuffs (according to the description of Capaccioni et al. 1995 and Szakács et al. 1998). The direct contact of the succession of the upper quarry yard and the sequence of the lower quarry yard is not exposed. The succession continues with a brownish, root cavity-bearing weathered zone, formed on a lithics-bearing, brown-colour volcanogenic sediment (layer A in Fig. 4a,b). The weathered zone is a well-known marker horizon identified in earlier studies (e.g. Capaccioni et al. 1995; Biró et al. 2017) Above it, with undulating erosional and topography-mantling contact,

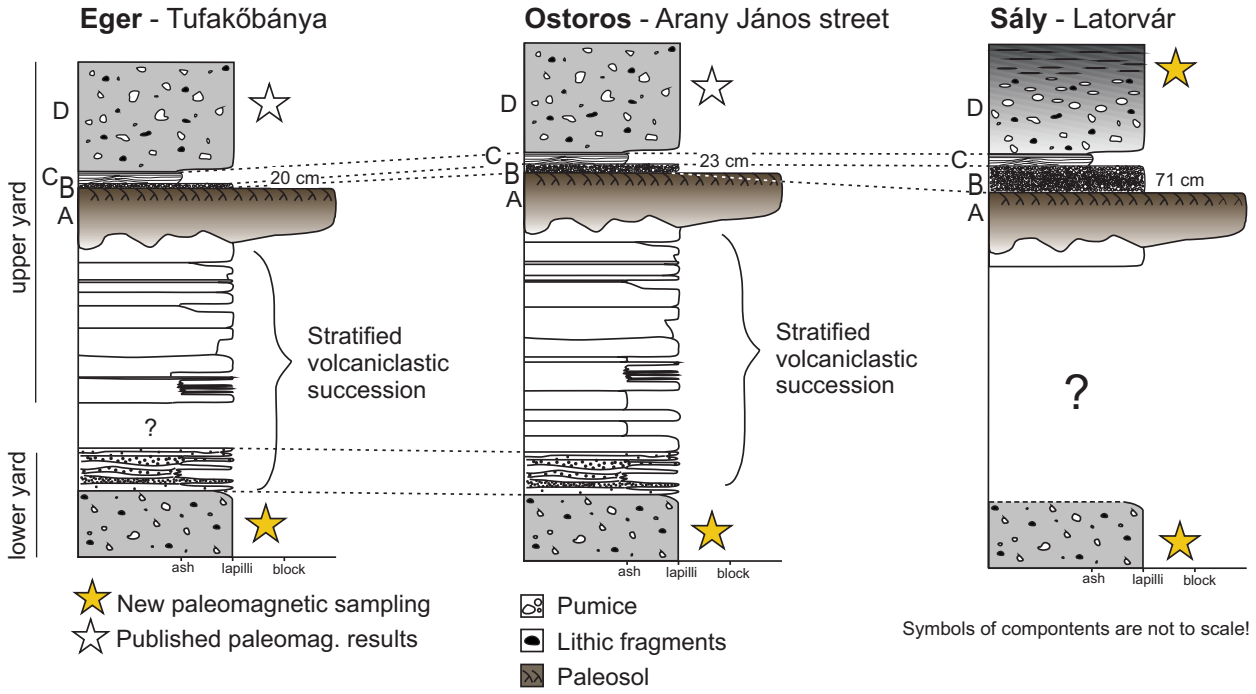

Fig. 3. Generalized lithostratigraphical column of the three investigated outcrops (except Szomolya). Note the increasing thickness of layer B of the Plinian sequence.

a well-sorted, 20 cm thick lapilli tuff (reported first by Capaccioni et al. 1995) can be observed, which follows a paleotopographic surface (layer B in Fig. 4a,b). The lapilli tuff is overlain by a 30 cm thick, undulating, cross-bedded, powder-like fine tuff horizon (layer C in Fig. 4a,b). This tuff bed is overlain (and separated with diffuse contact) by a ca. 20 m-thick massive, pumice- and lithic-bearing lapilli tuff (layer D in Fig. 4a,b). The phenocryst assemblage of the three mentioned deposits above the weathered zone (B to D) consists of quartz, biotite and plagioclase.

The succession of Ostoros – Arany János street consists of texturally diverse, internally complex assemblage of pyroclastic and reworked volcaniclastic deposits (Fig. 3). The lowermost unit is a poorly sorted, large pumice- (≥10 cm in diameter) and lithics-bearing lapilli tuff (Fig. 5b). Above this deposit a bedded volcaniclastic sequence crops out, overlain (as for Eger – Tufakőbánya, upper yard) by a complex stratified volcanic succession, which consists of several well-sorted lapilli tuffs or cross-bedded tuffs and reworked volcaniclastic deposits. On the top of this succession an easily identifiable, brown, weathered, 4–5 cm large lithic-bearing sediment crops out with clayish matrix and a well-visible weathered zone on the top (layer A in Fig. 5a). It is overlain by a 23 cm-thick, well-sorted lapilli tuff (layer B in Fig. 5a), which contains cm-sized pumices and mm-sized lithic fragments. Right above this lapilli tuff a few cm-thick fine tuff is exposed, which displays fine internal lamination, variable thickness (1–30 cm) and cross-bedding (layer C in Fig. 5a). Above it, a massive, poorly sorted, large pumice- (occasionally 10–15 cm in diameter) and lithics-bearing (up to 5–8 cm in diameter) lapilli tuff crops out (layer D in Fig. 5a), which shows weak cementation character after a few metres towards the top. The pumices are not flattened, but the rock itself becomes more compacted and harder upwards. The layers from B to D contain abundant biotite, plagioclase and quartz phenocrysts.

At the lowermost part of Latorvár hill, near the village of Sály next to the public road, a poorly sorted, massive, weathered, pumice-bearing lapilli tuff crops out with some cm-sized lithic clasts in the matrix (Fig. 3). This succession is heavily weathered, affected by recent soil formation (Fig. 6c). On the southern hillside, a well-visible, more than 1 m-thick, brown weathered zone is exposed, formed on a clayish brown volcaniclastic deposit (layer A in Fig. 6a). Above it, there is a 71 cm-thick, well-sorted, massive lapilli tuff horizon with pumice and lithic clasts (layer B in Fig. 6a). Unfortunately, this latter layer can be followed laterally only in a few metres. It is overlain by a white fine tuff showing laminated and sometimes cross-bedded internal structure (layer C in Fig. 6a). On the top of the succession, a pumice- and lithics-bearing, massive, non-welded lapilli tuff crops out, which changes upward in a few metres to welded lapilli tuff with 2–15 cm large fiamme structures and dense, grey matrix (Fig. 6b). At the lower level, undeformed white pumice clasts can be seen instead of fiamme (layer D in Fig. 6a). Phenocrystal assemblage of layer B to D consists of quartz, biotite and plagioclase.

At the eastern part of Szomolya village, a brown, clayish, sharp weathered zone occurs overlain by a well-sorted, coarse grained, clast-supported, pumice-bearing lapilli tuff, with variable thickness and, in some parts of the outcrop, an upper,

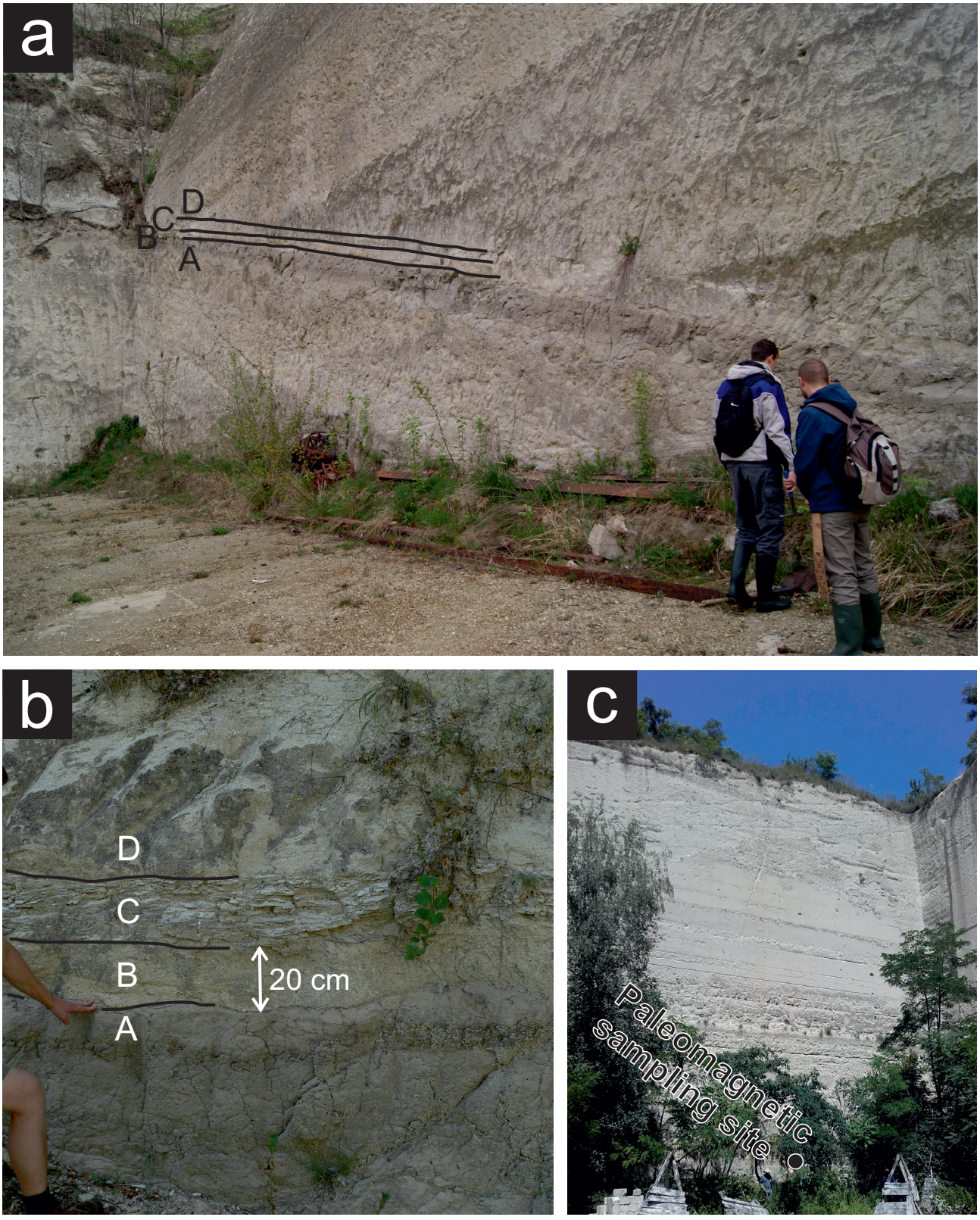

Fig. 4. Pyroclastic units of the Eger – Tufakőbánya site: **a** — the eastern wall of the upper quarry showing the upper part (including the Plinian succession) of the whole sequence (see chapter *Field observations* for explanation); **b** — the Plinian succession from a closer look; **c** — the lower quarry with the location of the paleomagnetic sampling site.

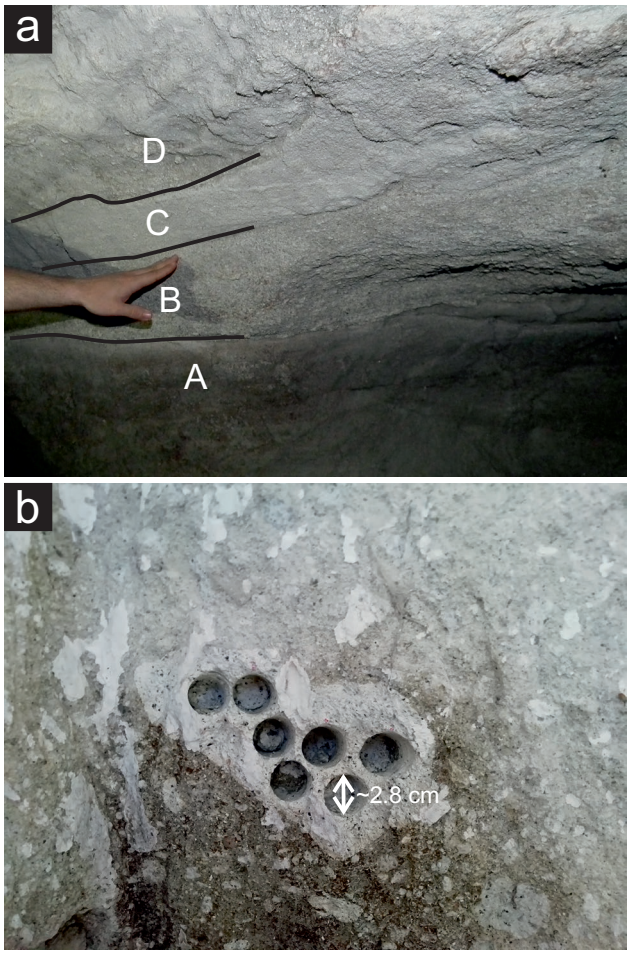

Fig. 5. The Plinian succession of the Ostoros – Arany János street site (**a**) and the paleomagnetic drilling holes within a pumice of the lower ignimbrite (**b**).

poorly sorted, pumice- and lithic-bearing, heavily weathered lapilli tuff cut into the well-sorted lapilli tuff reducing its thickness. The thickness of the well-sorted pyroclastic deposit can be well determined at 22 cm (Fig. 7). The whole outcrop is small-sized (<2 m in width) and heavily altered.

Granulometric characteristics of layer B

The results of the granulometric measurements are summarized in Table 2.

At Eger – Tufakőbánya the well-sorted lapilli tuff, deposited on top of the brown weathered zone, does not contain significant amount (~5 % by visual estimates) of lithic clasts; rather, altered pumices are abundant. The phenocryst assemblage is dominated by idiomorphic bipyramidal or fragmented quartz crystals. The largest lithic fragment measured is 6.9 mm in diameter; the average diameter of the five and ten largest lithics is 5.6 mm and 4.4 mm, respectively. The largest quartz phenocryst is 3.4 mm in diameter, but there is no significant variability in size, thus the diameter of the five and ten largest quartz phenocrysts is almost the same (3.2 mm and 2.9 mm, respectively).

At the southern part of the wine cellars in Ostoros, again both the brown weathered zone and the sampled well-sorted lapilli tuff on its top crops out. The largest lithic clast measured at this site is 6 mm, whereas the diameter of the largest quartz phenocryst is 3.2 mm in diameter. The quartz phenocrysts are dominantly idiomorphic; the original bipyramidal shape can be observed in case of the quartz fragments, too. The average diameter of the five and ten largest lithic clasts is 5.4 mm and 4.7 mm, respectively. Similarly to the other site, the five and ten largest quartz phenocryts are of the same size (3.1 mm and 3 mm in diameter, respectively).

At Sály – Latorvár, also the well-sorted lapilli tuff sitting on top of the brown weathered zone was sampled. In contrast to the other two sites, this lapilli tuff horizon is heavily weathered, the pumices almost disappeared, and the matrix is brownish in colour. The lithic clasts and quartz phenocrysts are much less weathered. The largest lithic fragment is 15.7 mm, and the largest quartz phenocryst is 4 mm in diameter. The quartz phenocrysts are idiomorphic with bipyramidal shape, but often cracked or fragmented. The average diameter of the five and ten largest lithics is 8.2 mm and 6.4 mm, respectively, whereas the average diameter of the five and ten largest quartz phenocrysts is 3.3 mm and 3 mm, respectively.

To summarize the field observations and granulometric results, one of the most important parameters of the fall layer we can use for the determination of the location of the eruption centre is its thickness. The correlated pyroclastic fallout layers show different thickness at the three sites: Eger – Tufakőbánya: 20 cm, Ostoros – Arany János street: 23 cm, Sály – Latorvár: 71 cm. Thickness of the fallout layer of the additional site was also taken into account at Szomolya where the same fallout layer is measured to be 22 cm thick. The maximal and average diameters of the lithic clasts were also used to estimate the direction of the coarsening of the pyroclastic fallout layer. The measured maximal lithic diameters in each site are the following: Eger – 6.9 mm, Ostoros – 6 mm, Sály – 15.7 mm. We calculated the mean diameter of the five (Eger: 5.6 mm, Ostoros: 5.4 mm, Sály: 8.2 mm) and ten (Eger: 4.4 mm, 4.7 mm, 6.4 mm) largest lithics (Table 2).

Paleomagnetism

The demagnetization experiments revealed that the NRM of the strongly welded ignimbrite from Sály – Latorvár (upper, acc. to. Table 1) has practically a single component NRM, yielding the same paleomagnetic direction duing AF and thermal demagnetization (Fig. 8A–C). The NRM is practically lost by the Curie point of magnetite while the susceptibility moderately increases from 150 °C upwards (Fig. 8C). The non-welded material (Sály – Latorvár, lower) below the strongly welded horizon behaves differently on AF and thermal demagnetizations, respectively. The direction remains stable on AF demagnetization, (Fig. 8D and E), while moves along a great circle on thermal demagnetization the paleomagnetic direction

changes (Fig. 8F) and moves along a great circle (Fig. 8E), indicating the composite nature of the natural remanent magnetization. The samples from Eger – Tufakőbánya (lower yard) and Ostoros (lower) exhibit identical paleomagnetic properties to the non-welded horizon at Sály – Latorvár (lower), i.e. the paleomagnetic directions become more and more scattered with increasing temperature on thermal demagnetization (Fig. 9 D–F, G–I, J–L). These observations, together with the 'co-existence' of normal and reversed polarity direction, makes highly unlikely that the remanence was acquired during cooling. Moreover, the paleomagnetic directions from Eger – Tufakőbánya (lower yard) (Fig. 8G–I) and from Ostoros – Arany János street (lower) (Fig. 8J–L) are incompatible with the acquisition of the remanence during fast cooling, which excludes the co-existence of both normal and reversed polarity primary magnetizations at a given site.

Based on the behaviour of the pilot samples on thermal demagnetization, we selected 300 °C and 500 °C steps for

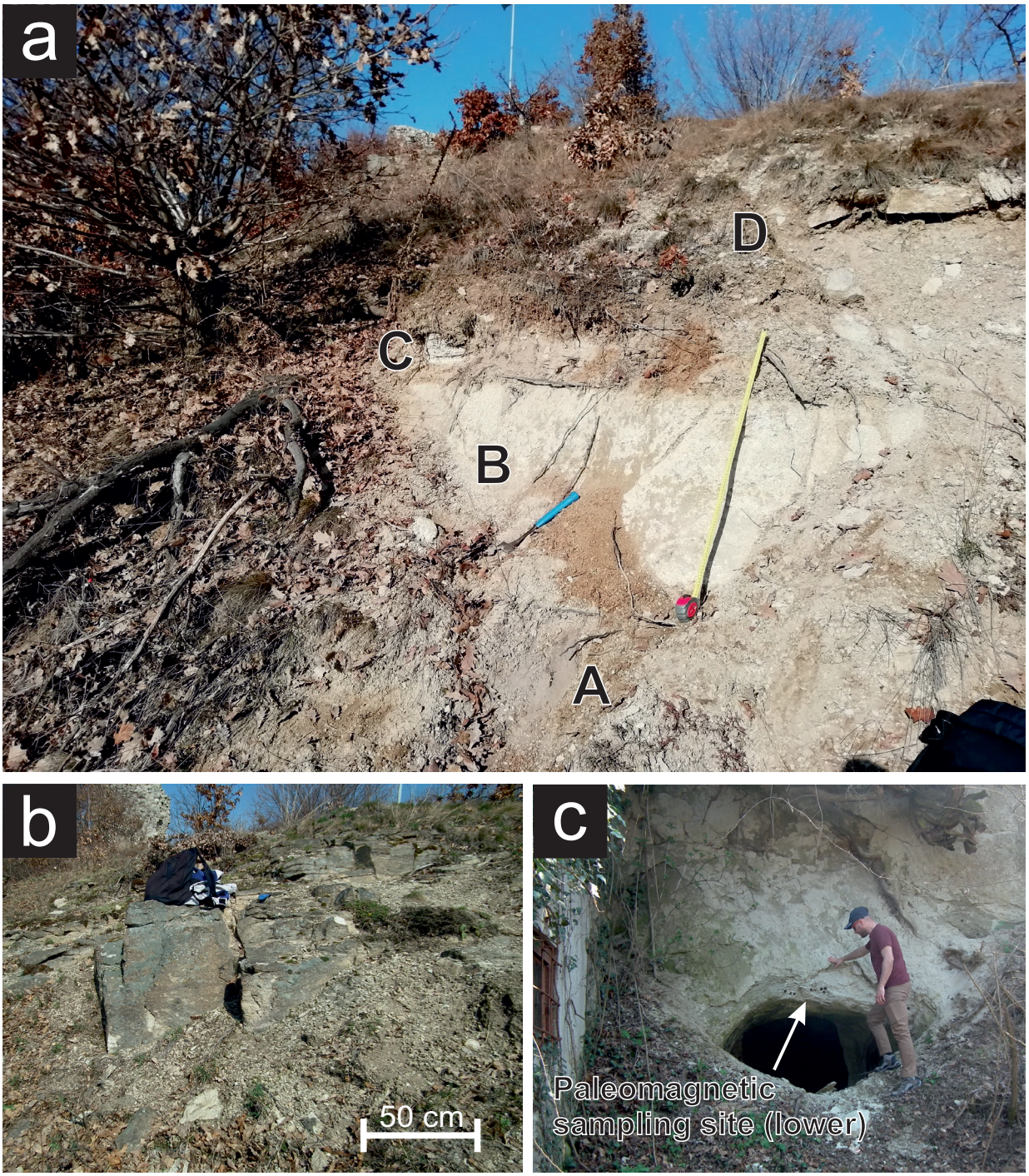

Fig. 6. The Plinian succession (**a**) and the lower ignimbrite at the Sály – Latorvár site (c).

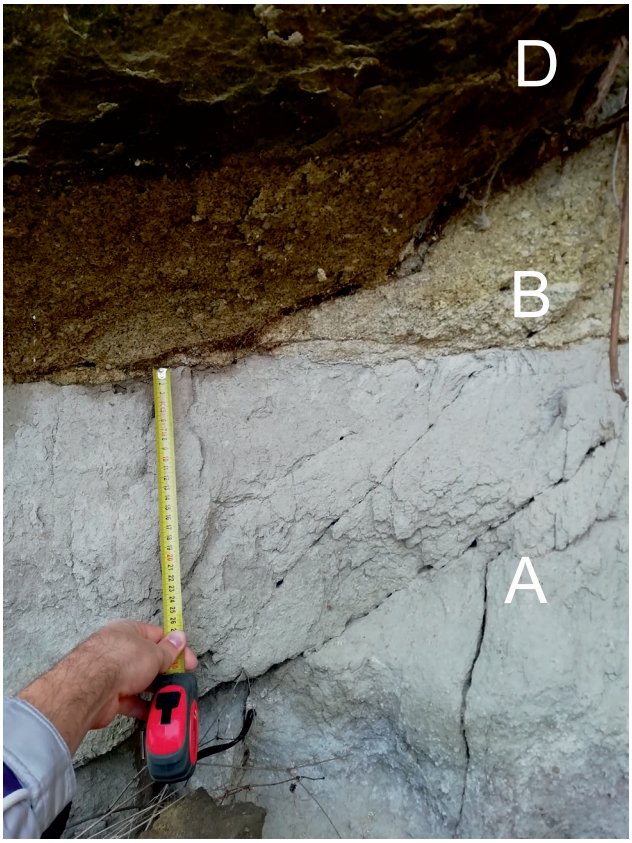

Fig. 7. The Plinian succession at Szomolya. Note that layer C is eroded here.

documenting the change in scatter of the individual paleomagnetic directions. In all cases the scatter of the individual directions increases with the temperature (Fig. 9D–L), which is the opposite of the trend exhibited by strongly welded ignimbrites having very stable NRM and reacts with improving scatter to both AF and thermal demagnetization (Figs. 8A–C, 9A–C, for more evidence the reader is referred to Márton & Márton 1996).

An interesting aspect of the sampled non-welded ignimbrites is that the component removed during demagnetization has similar directions in most samples from the same site (Table 3). This component could have been imprinted during the eruptions of the welded Middle Pyroclastic Complex by a moderate re-heating, as the declinations (320–335°) fit to the rotation indicated by this complex (Márton & Márton 1996). After the removal of this overprint remanence, the NRM directions became scattered and chaotic, which implies that the sites in question probably never had primary uniform magnetizations.

By contrast, the welded ignimbrites or massive, cemented lapilli tuffs from higher stratigraphic positions at the same locations (e.g. Sály – Latorvár, upper) have reversed polarities and suggest much larger CCW rotation (Table 3). These sites satisfy the criteria for primary magnetization acquired during cooling from high temperature (see Fig. 9A–C). Such ignimbrites were emplaced at high temperatures and they were clearly not sensitive to the heating effect of the subsequently erupted Middle Pyroclastic Complex.

Discussion

Interpretation of the pyroclastic succession

Based on the identical phenocryst assemblage of the fallout – ground surge – ignimbrite succession and the lack of erosional signals between the mentioned layers we assume that these deposits should represent various phases of the same eruption (cf. Fierstein & Hildreth 1992; Wilson 1993; Druitt 1998; Vespa et al. 2006). Thus, if the source region of the pyroclastic fallout layer can be determined, it must be considered as a source for the whole succession, including the PDC-laden material too.

Both the lower and upper, poorly sorted, massive, pumice-bearing lapilli tuff which crops out at all three sites (Eger, Ostoros and Sály, Fig. 3) can be interpreted genetically as an ignimbrite. Ignimbrites form during large-volume, explosive volcanic eruptions, when the eruption column becomes unstable due to the decrease of the buoyancy and the widening of the volcanic conduit (Wright & Walker 1981; Walker 1983; Valentine 2020). Welding is a common feature in the case of ignimbrite accumulation, when the deposit is subjected to sufficiently high pressure and persistently high temperature that enables to retain heat to cause welding immediately after the accumulation of the pyroclasts. The welding process is commonly enhanced or facilitated by fluid migration into the fast depositing porous pumiceous pyroclastic piles from the underlying sediments (Branney & Kokelaar 1992; Pioli & Rosi 2005; Randolph-Flagg et al. 2017).

The observed brown-coloured weathered zone (layer A, Figs. 3, 4, 5, 6, 7) with irregular surface is interpreted as a paleosol, as suggested by the crumbly, clay-rich appearance and brown colour. Moreover, at Eger – Tufakőbánya a 40 cm long

Table 2: The result of the granulometric measurements for the investigated sites.

Site	Largest lithoclast (mm)	Largest quartz phenocrystal (mm)	Mean size of the five largest lithics (mm)	Mean size of the ten largest lithics (mm)	Mean size of the five largest quartz phenocrysts (mm)	Mean size of the ten largest quartz phenocrysts (mm)
Eger – Tufakőbánya	6.9	3.4	5.6	4.4	3.2	2.9
Ostoros – A. J. street	6	3.2	5.4	4.7	3.1	3
Sály – Latorvár	15.7	4	8.2	6.4	3.3	3

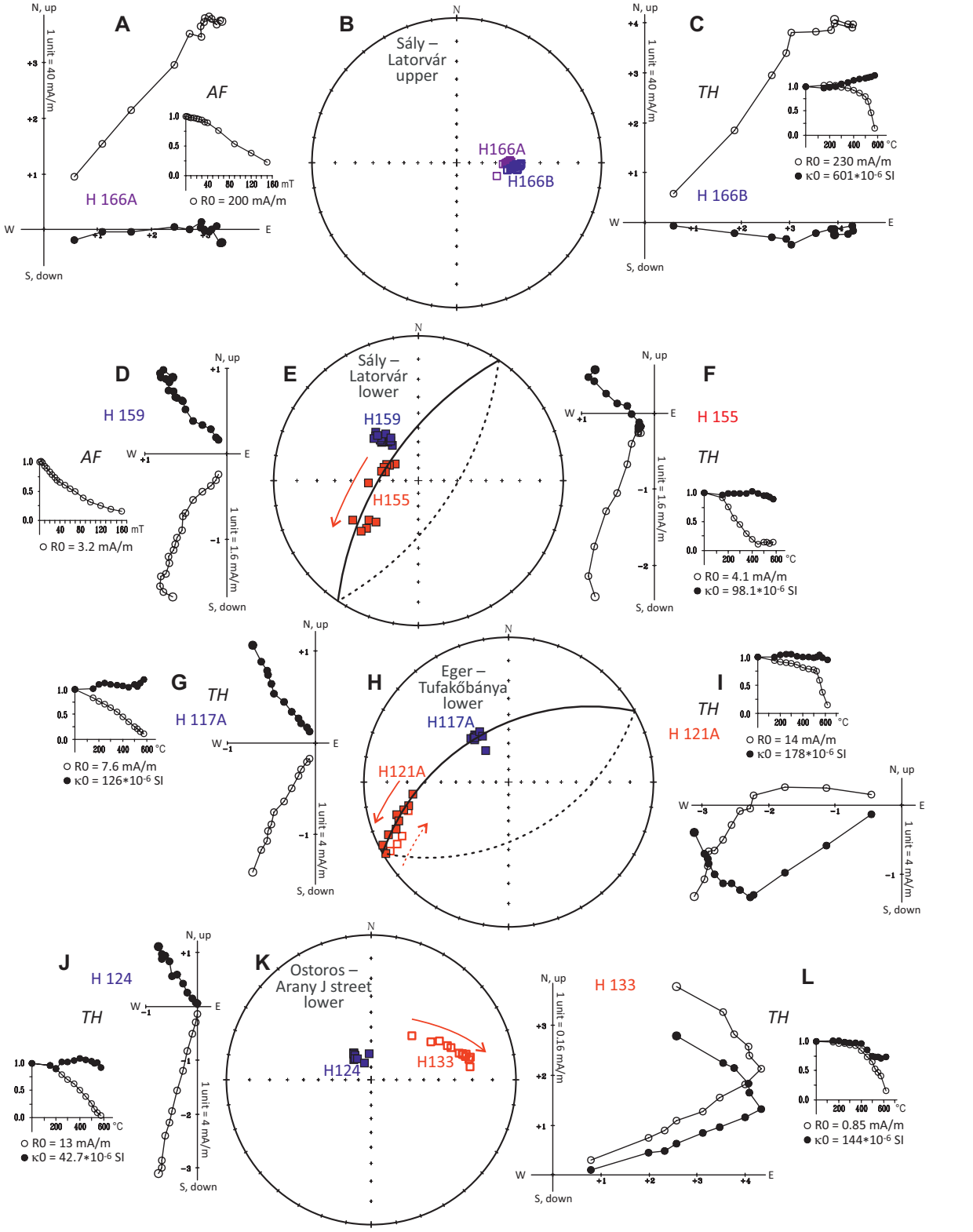

Fig. 8. Typical demagnetization behaviour of pilot samples from Sály – Latorvár upper, strongly welded ignimbrite (**A–C**) from the same location from non-welded tuff (lower, **D–F**), from Eger – Tufakőbánya, lower yard (**G–I**) and from Ostoros – Arany János street lower (**J–L**). Demagnetization curves on the left and right sides, respectively show samples from the same site. Their directions change on demagentization is compared in stereographic projections in the middle column. Key: Zijderveld diagrams (A, C, D, F, G, I, J and L) are in the geographic system and are accompanied by intensity (circles) versus demagnetizing field diagrams, when the method of demagnetization is AF, and by NRM intensity (circles)/susceptibility (dots) versus temperature diagrams, when the method of demagnetization is thermal. In the Zijderveld diagrams full dots are the projections of the NRM vector onto the horizontal, circles: into the vertical.

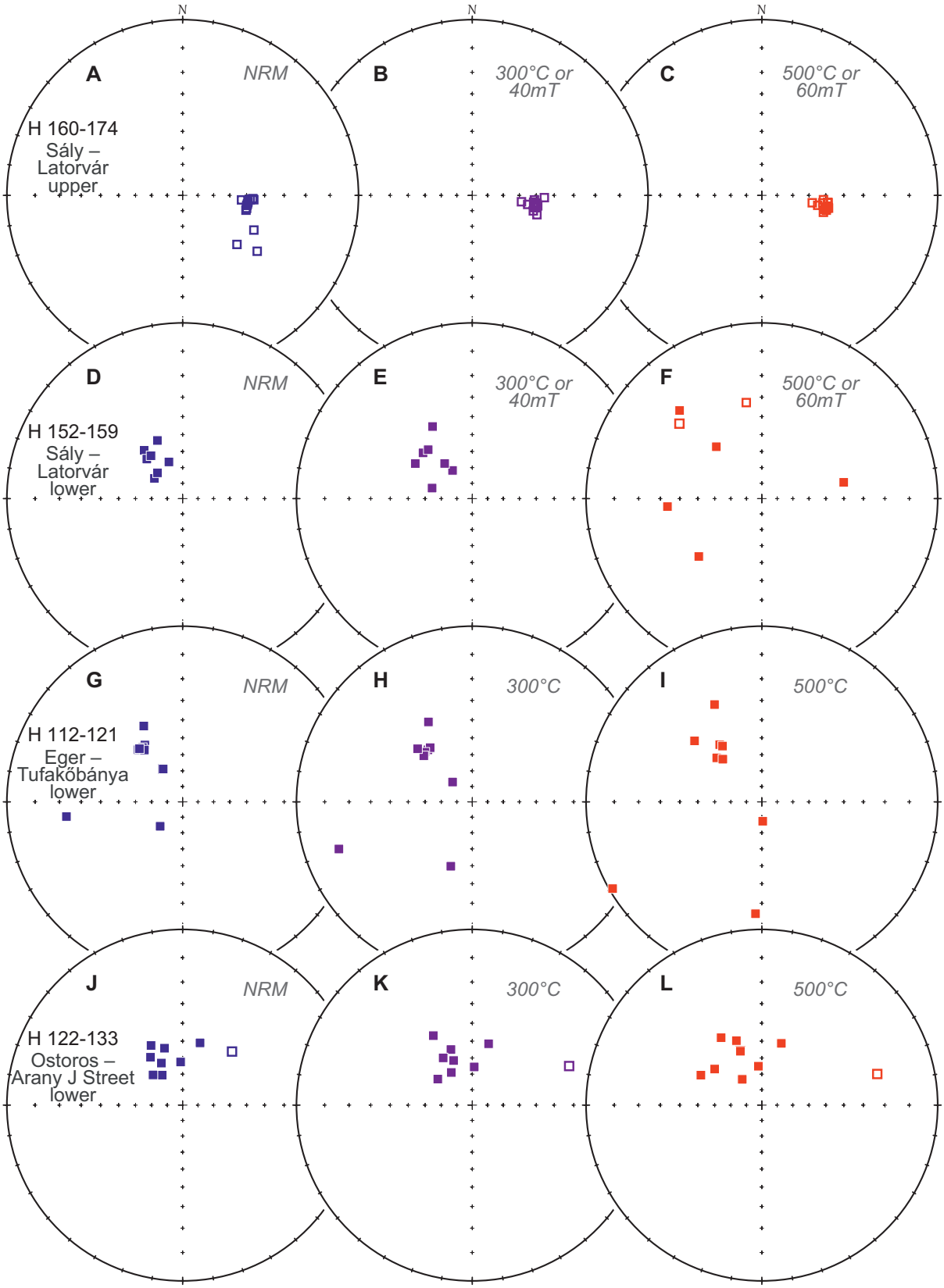

Fig. 9. Comparison of the grouping of the magnetic directions of the individual samples before demagnetization (NRM), measured after 300 °C (and some at 40 mT AF demagnetization) and after 500 °C (and some at 60 mT AF demagnetization). The sites are Sály – Latorvár, upper (**A–C**) and lower (**D–F**), Eger – Tufakőbánya, lower yard (**G–I**) and Ostoros – Arany János street, lower (**J–L**). Key: full symbols — N polarity; hollow symbols — R polarity magnetizations.

Table 3: Summary of locality mean paleomagnetic directions for the study area. The mean directions for sites 1 and 3 are based on the linear segments of the demagnetization (Kirschvink 1980) which decay towards the origin of the Zijderveld diagrams, for site 6 on the linear segments which start to decay from the direction before demagnetization (note that such component was found only at seven out of the 12 samples), for sites 4 and 5 it is the combination of components starting to decay from the direction before demagnetization and the components derived from remagnetization circles (McFadden & McElhinney 1983). Key: Lat. N, Lon. E — Geographic coordinates (WGS84); n/no — number of used/collected samples (the samples are independently oriented cores); D, I — declination, inclination; k and α95: statistical parameters (Fisher 1953).

	Locality	Lat. N, Lon. E	alt. (m)	n/no	D°	I°	k	α_{95} °	reference
Welded/cemented ignimbrites, Primary magnetizations									
1	Ostoros – Arany J. street, upper 6019–6024	47°51'35" 20°26'22"		6/6	122.4	−47.0	104.2	6.6	Márton & Márton 1996, updated
2	Eger – Tufakőbánya, upper yard 6308–6312	47°53'01" 20°24'18"		5/5	115.1	−55.3	86.4	8.3	Márton & Márton 1996
3	Sály – Latorvár, upper H 160–174	47°58'44" 20°38'26"	243	14/15	94.8	−52.5	490.7	1.8	this paper
Non-welded ignimbrites, Overprint magnetizations									
4	Sály – Latorvár, lower H 152–159	47°58'52" 20°38'08"	212	7/8	321.8	59.1	537.8	3.0	this paper
5	Eger – Tufakőbánya, lower yard H 112–121	47°53'09" 20°24'00"	182	9/10	320.0	49.3	169.7	4.2	this paper
6	Ostoros – Arany J. street, lower H 122–133	47°51'47" 20°26'18"	171	7/12	334.1	58.4	76.9	6.9	this paper

calcified root tube was found inside the same horizon, confirming further its paleosol origin. Paleosols are formed in terrestrial settings during extended (e.g. years- to millenia-long) periods of dormancy between volcanic phases (e.g. Wilson et al. 2001) when the environmental/climatic conditions are stable, allowing significant weathering (e.g. Solleiro-Rebolledo et al. 2003).

Above the paleosol, with erosional contact, a well-sorted, pumice-bearing, mantle-bedded lapilli tuff with laterally constant thickness crops out (Figs. 3, 4, 5, 6, 7). It is interpreted as a pyroclastic-fallout deposit on the basis of its mantle bedding and reasonably good sorting. It is inferred to have been deposited during the initial phase of a Plinian eruption, when the eruption column was still stable (Walker 1971; Streck & Grunder 1995). The cross-bedded, whitish fine tuff on top of the fallout deposit suggests a dilute ground surge formed as part of the following PDC phase, when the eruption column started to collapse (Fisher 1979; Druitt 1998). This PDC deposit is followed upwards by the upper ignimbrite with a diffuse transition, as can be observed both at Eger and Ostoros (Figs. 4, 5). The pyroclastic fallout – dilute PDC – ignimbrite deposit sequence is well-documented and observed worldwide, and interpreted as resulting from Plinian-type eruptions where a complete column collapse occurs in the paroxysmal phase of the eruption (Sparks et al. 1973; Fisher 1979; Fierstein & Hildreth 1992; Wilson 1993; Druitt 1998; Vespa et al. 2006).

Correlation of the pyroclastic units

The pyroclastic successions examined at the three sites can be correlated on the basis of the following features (Fig. 3): 1) the same continuous sequence with the same vertical order (layer A to D): paleosol – pyroclastic fallout layer – deposit from a dilute, turbulent PDC – ignimbrite, which are observed everywhere; 2) the textural features observed at outcrop scale (e.g. bedding types, grain size variations, componentry etc.) are nearly the same in all three outcrops; there are only subtle differences in the grain-size characteristics, the thickness of certain units, and the degree of welding of the upper ignimbrite; 3) the paleomagnetic properties of the lower ignimbrite are similar in all three cases, i.e. they do not seem to have had uniform NRM imprinted during deposition (Fig. 9), while the capping ignimbrite at all sites preserved their primary NRMs fitting to those of the LPC in the BFVA (Fig. 9 and Márton & Márton 1996). In summary, the lower ignimbrite of the succession can be classified as belonging to the Eger ignimbrite unit, whereas the upper one belonging to the Mangó ignimbrite unit (as named by Lukács et al. 2018).

It is important to note, that despite the fact that the lithostratigraphic column of Sály – Latorvár (Fig. 3) is not continuous, it correlates well with the succession of other two sites based on the lithological characteristics of the exposed layers and their paleomagnetic features (Fig. 3). Moreover, it also has to be highlighted, that although the Szomolya succession was not investigated in detail, its field volcanology properties and stratigraphical position (based on Szakács et al. 1998; Lukács et al. 2005) suggest that the latter sequence shows the same succession as that of Eger, Ostoros and Sály.

The new paleomagnetic result from the upper, welded ignimbrite from Sály – Latorvár (upper) shows large (85°) CCW rotation, similarly to the earlier studied Eger – Tufakőbánya (upper yard) and Ostoros – Arany János street, upper (Mangó ignimbrite unit, Table 3). All of them can be classified as still belonging to the LPC, too. The ignimbrite of the Eger ignimbrite unit is situated in lower position in the stratigraphic column than the ignimbrite of the Mangó ignimbrite unit, therefore it has to be also part of the LPC. Although primary

NRM could not be recognized in the three studied sites of the Eger ignimbrite unit, correlating them is justified by their common magnetic – paleomagnetic features, like weak susceptibilities and weak remanent magnetizations imprinted possibly during the emplacement of the Middle Pyroclastic Complex (which shows similar 30° declinations, cf. Márton & Márton 1996 and Márton & Pécskay 1998).

Clues for an eastward-located source region

Pyroclastic-fall deposits are good candidates to help identifying the source region based on the systematic variation of their thickness and grain-size characteristics with distance from the eruption centre (e.g. Wilson 1993). However, during a volcanic explosive eruption strong, uni- or multi-directional winds can alter the expected regular asymmetric tephra dispersal pattern, so that:

- isopachs are often elliptic in shape around the eruption centre with the long axis oriented in the dominant wind direction (Sparks et al. 1992);
- moving away from the eruption centre the thickness of a fallout layer is not strictly monotonously decreasing in all directions (Houghton et al. 2014); in addition, a PDC deposit emplaced directly on top of soft, unconsolidated pyroclastic fallout deposit very often cuts into the latter and reduces the thickness of the fallout deposit at different site-specific manner (Sparks et al. 1997);
- the well-sorted grain-size distribution of a fallout layer can also be modified and spoiled because intervening strong winds can disperse the particles in a way other than predicted (Sparks et al. 1992). In particular, in crystal-rich fallout products, crystals often have restricted size and density ranges. Crystal enrichment may occur at medial or distal localities causing bimodal grain-size distribution of the deposits (Sparks et al. 1992). In contrast, the strictly monotonous decrease of the diameter of the largest lithoclasts with distance from the eruption centre is only rarely modified (Mele et al. 2020). The lithics, having higher density, fall out from the eruption column earlier and closer to the vent, so their size will be the largest in proximal settings (Campbell et al. 2013). In the case of the examined sites in this work, this observation is confirmed: the size of the largest quartz phenocrysts does not scatter significantly, the average values are respectively the same at all localities.

In our study the largest lithoclast was found in the fallout deposit at Sály – Latorvár, exceeding the values of the other two outcrops (Table 2). More lithics larger than 5 mm in diameter were measured at Sály – Latorvár, than in the other two occurrences (Table 2). Therefore, the typical mean lithoclast-diameter of the ten largest clasts was higher at Sály, than at Eger and Ostoros.

The thickness of the fallout layer is progressively increasing towards the east (Figs. 3 and 10). There are no any signs of post-emplacement reworking of the tephra or thickness reduction due to the erosional effect of the overlying ignimbrite (except at Szomolya), thus we consider the measured thicknesses as representing the original primary thickness of the fallout deposit. The significant and systematic increase of the thickness from west (Eger – Tufakőbánya) to east (Sály – Latorvár) (plot in Fig. 10) suggests a roughly eastward directed (including also northeastern or southestern) origin of the investigated fallout horizon (layer B) (Fig. 10). The thickness of the fallout layer cropping out at Szomolya is in good agreement with the observation stated above, as fitting respectively to the trend of the bed thickening toward east (Fig. 10). Thus, the increasing thickness of the fallout layer is accompanied by a similar increase of the mean diameter of the largest lithic clasts towards the east, which suggests a westward transportation of the pyroclasts (Fig. 10). An additional field observation is that the ignimbrite of the Mangó ignimbrite unit is densely welded in the easternmost outcrop (Sály – Latorvár), which also supports its closer relative position to the source area (cf. Streck & Grunder 1995). However, welding of ignimbrites is also significantly controlled by the syn-eruptive topography (Walker 1983), consequently the presence of one welded ignimbrite facies is not unequivocally a consequence of more proximal position. In this respect, we note that the source region was suggested in the vicinity of Miskolc (Lukács et al. 2010) based on the variation of thickness and welded facies of ignimbrites in the Miskolc-7, Miskolc-8 and Nyékládháza-1 boreholes (M-7, M-8, Nyh-1 in Figs. 2 and 10*,* Lukács et al. 2010). Another eruption centre was inferred earlier to the vicinity of Mezőkövesd (Fig. 2), but for the Middle Pyroclastic Complex instead of LPC (Szakács et al. 1998).

Confirmation of an eastward source region based on isopach patterns of Plinian eruptions

The distance of the eruption centre can be tentatively inferred by the largest thickness of the fallout layer; however, in proximal areas the thickness of fallout horizons can range from a few tens of cm to several m depending on the magnitude of the eruption and the wind direction at the time of the eruption. For comparison, largest thicknesses in most proximal accessible locations: 180 cm for Taupo AD 186, New Zealand (Walker 1980); 99 cm for Pululagua, Ecuador (Papale & Rosi 1993); 140 cm for Quilotoa, Ecuador (Mothes & Hall 2008); 53 cm for Late Bronze Age Santorini LP2-A2 unit, Greece (Simmons et al. 2017). Considering these thickness values, although the exact position of the eruption centre cannot be determined, the source region could be relatively close with regard to the largest thickness values of our studied pyroclastic fallout deposit (71 cm): ca. 5–15 km eastward from the easternmost site (Sály – Latorvár). It has to be pointed out, that the "eastward" means here that the source region was located toward the east (including northeast and southeast) from the BFVA in a larger area, not exactly the east. We considered two hypothetical source areas: an easterly at the vicinity of Miskolc, and a southerly at the vicinity of Mezőkövesd (Figs. 11, 12). The Bükk Mountains in the northern vicinity of the BFVA mainly consists of Mesozoic limestone without any Miocene igneous bodies according to the detailed geological

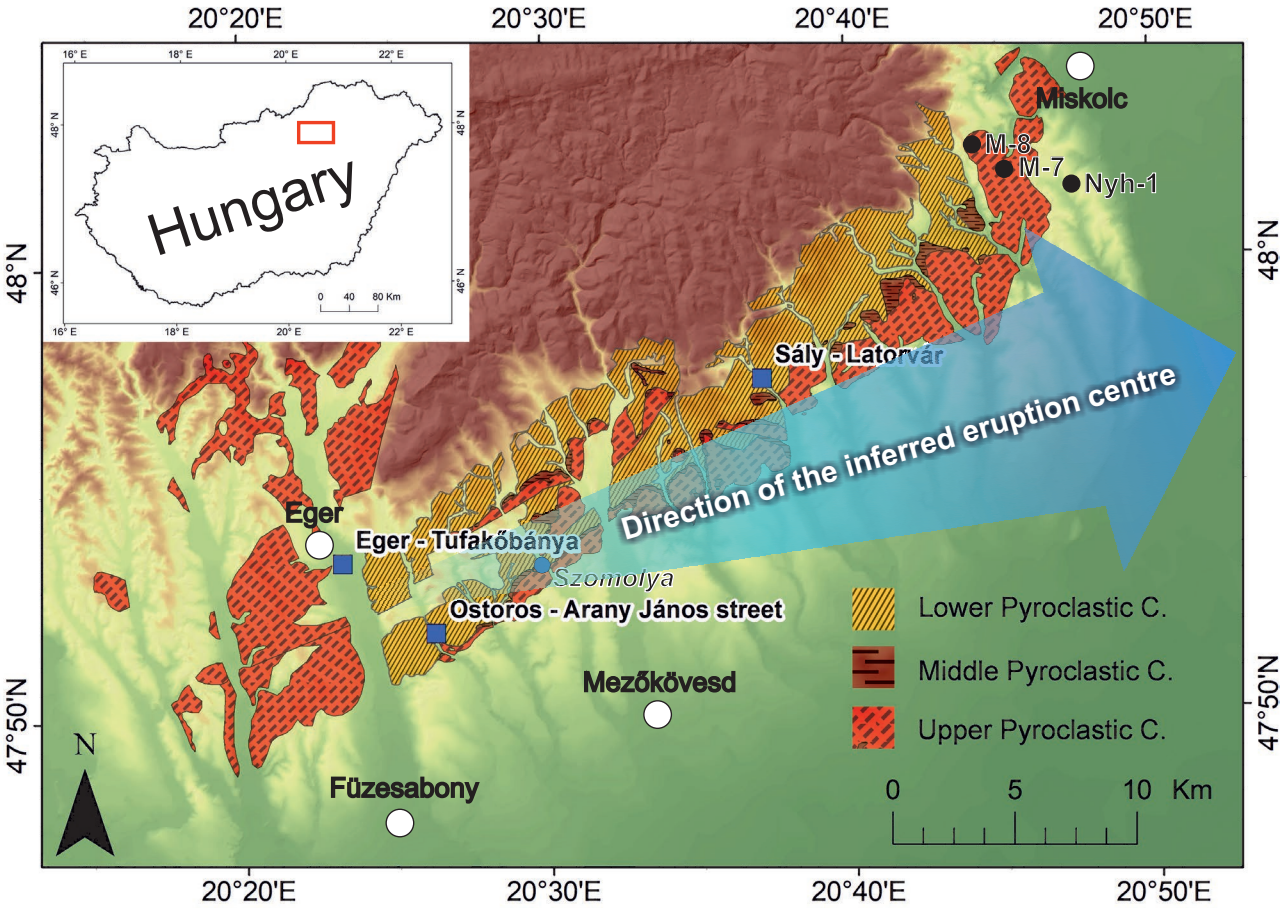

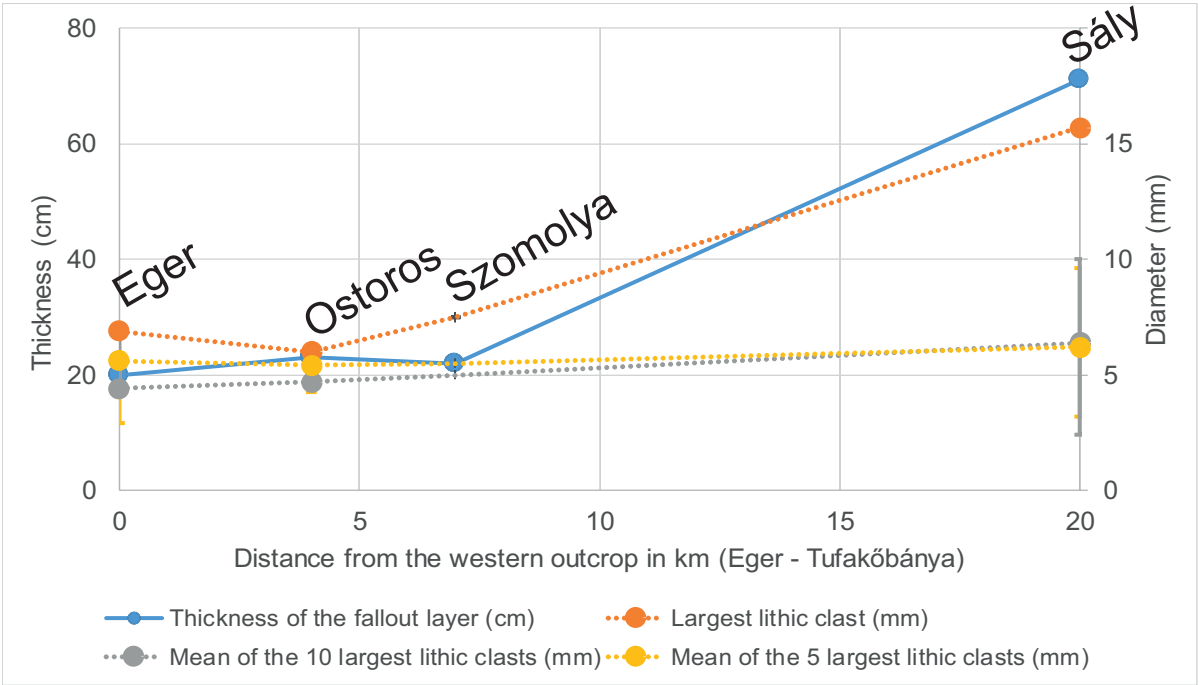

Fig. 10. The possible provenance direction of the investigated Plinian sequence based on the thickness and granulometric properties of layer B. Lower plot: Thickening and coarsening data as a function of distance from the Eger – Tufakőbánya site. Error bars were calculated by considering the standard deviation of each measured populations.

mapping (https://map.mbfsz.gov.hu/fdt100/), thus this region cannot be considered as a potential source area of the investigated pyroclastic succession.

In order to test the reality of the two possible configurations, dispersal patterns revealed by isopach systematics of four different, well-studied Plinian eruptions worldwide were chosen (Figs. 11, 12), where fallout tephra could have been identified and mapped, hence a reliable and complete isopach map was drawn. The criteria of the selection were the followings: 1) the presence of Plinian or sub-Plinian eruptions; 2) complete isopach lines based on a great number of sampling points; 3) representation of various wind conditions (especially wind direction and strength) under which between the chosen eruptions occurred. Thus, the four eruptions called here for comparison are the following (from 'a' to 'd' according to the notations in Figs. 11, 12): a, Pululagua Plinian eruption, Ecuador, 2450 BP – no-wind condition (Papale & Rosi 1993); b, Masaya Tuff, Nicaragua, 3000–6000 BP – light wind condition, Plinian–Phreatoplinian-type eruption (Bice 1985); c, Hekla Plinian eruption, 1104 CE – strong one-way wind (Janebo et al. 2016); d, Unit E (Opepe Tephra), 9050 BP – Taupo volcano, New Zealand – similar geotectonical setting and eruption style like in the case of the BFVA (Wilson 1993).

The isopach maps of these reference eruptions were re-sized to the same scale as our study area (implying slightly or significantly different-scale tephra dispersal relative to the BFVA) and then they were digitized. The obtained dispersal pattern was added to the BFVA map with the above mentioned two hypothetical eruption centres as "end members" within the possible source area (Figs. 11, 12). It is noteworthy, that Masaya and Hekla are more mafic (Bice 1985; Janebo et al. 2016), hence the density and vesicularity of their pyroclasts differ from the felsic and highly vesicular pyroclasts in our case.

When an eastern source area is considered, the no-wind scenario which dominated the Pululagua eruption limits the areal extent of the fallout activity (Fig. 11a). In this case, the BFVA outcrops which were investigated are seemingly too far from the centre, and it is unrealistic to reach 70 cm thickness in

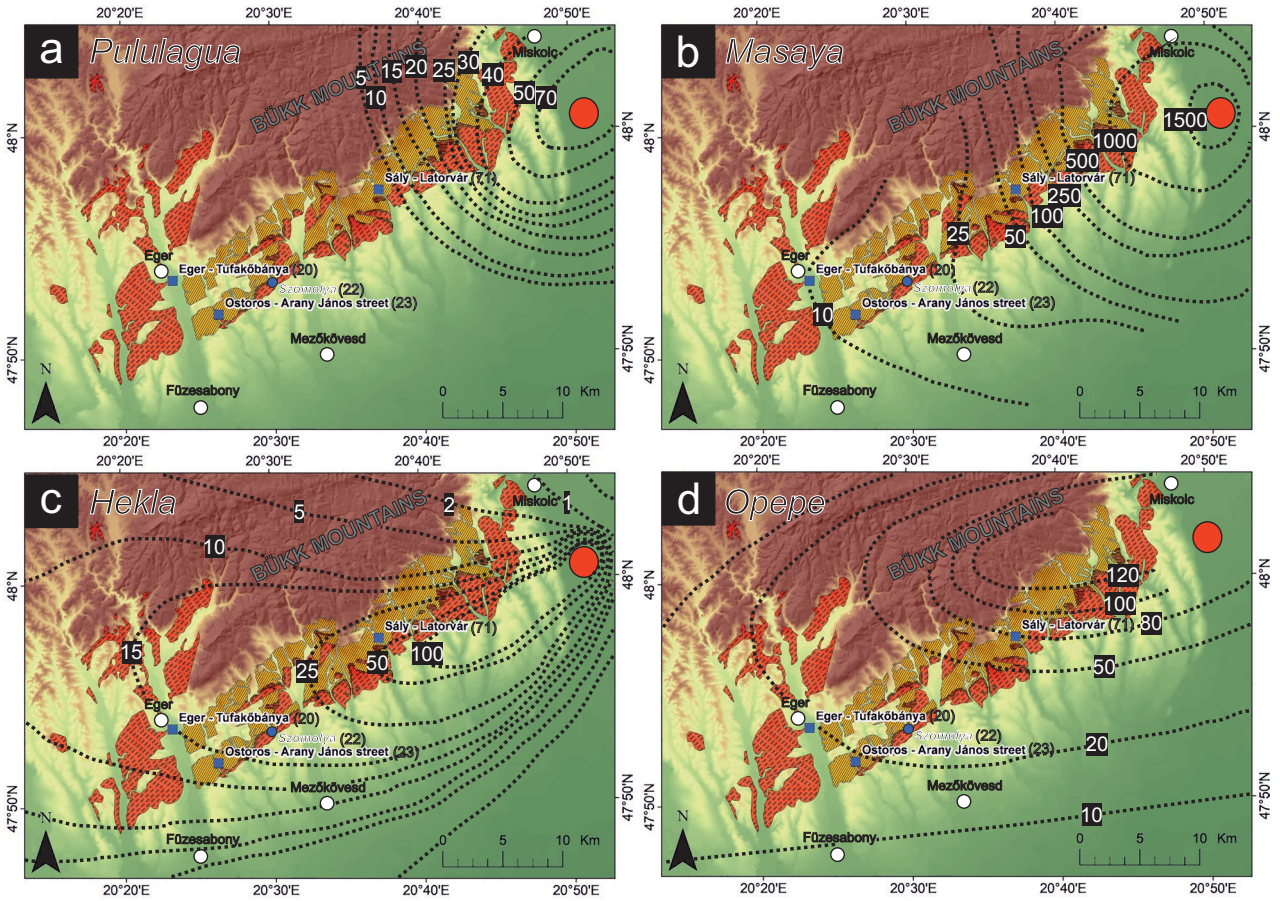

Fig. 11. Scaled isopach maps of selected Plinian fallout tephra fitted to a possible eastward located source vent. Note the remarkable correspondence of the measured thickness data and the isopach map on c and d. **a** — Pululagua Plinian eruption, Ecuador, 2450 BP – no-wind condition (Papale & Rosi 1993); **b** — Masaya Tuff, Nicaragua, 3000–6000 BP – light wind conditions, Plinian–Phreatoplinian-type eruption (Bice 1985); **c** — Hekla Plinian eruption, 1104 CE – strong one-way wind (Janebo et al. 2016); **d** — Unit E (Opepe Tephra), 9050 BP – Taupo volcano, New Zealand – similar geotectonical setting and eruption style like in the case of the BFVA (Wilson 1993). The measured thickness of layer B in brackets. All values are in cm.

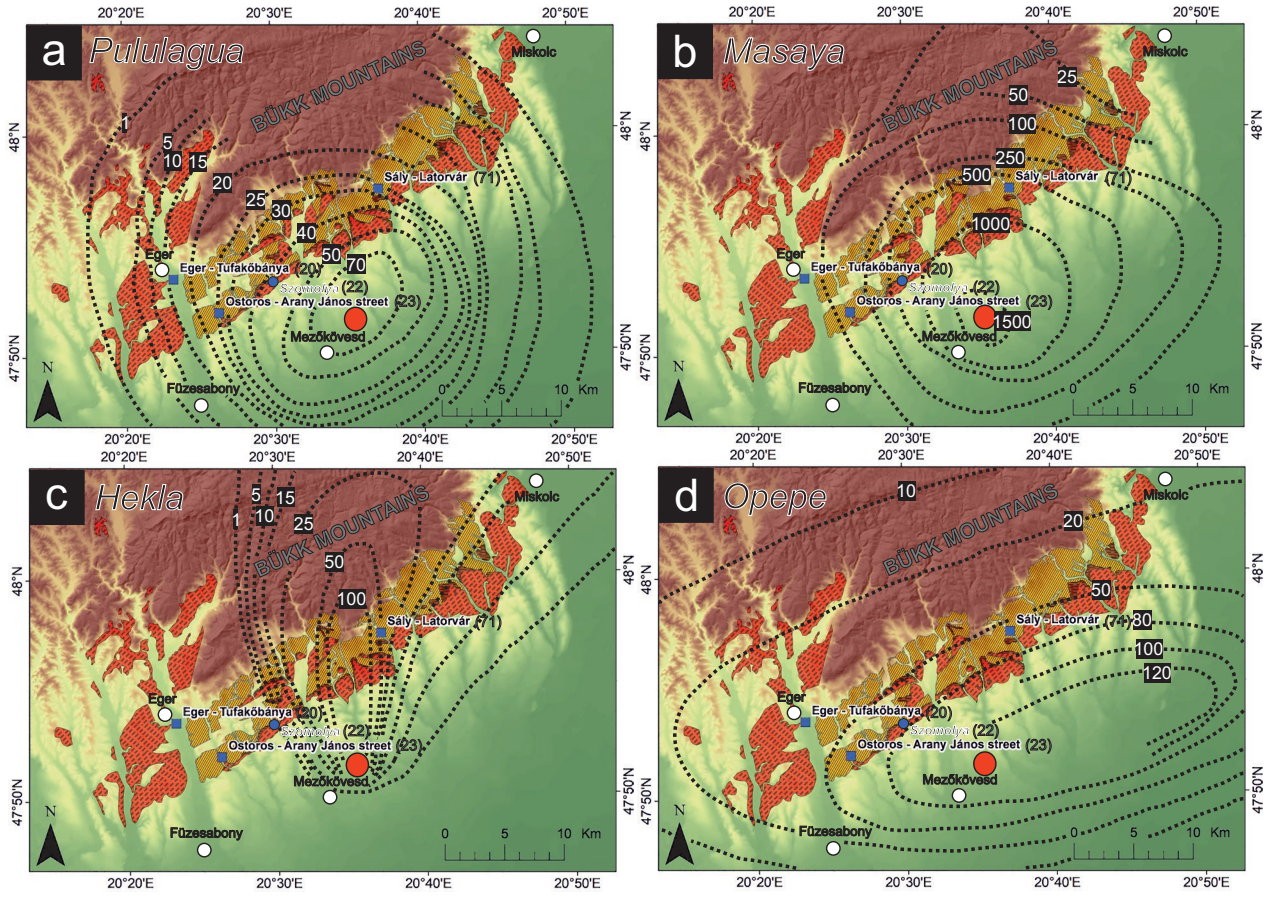

Fig. 12. Scaled isopach maps of selected Plinian fallout tephra fitted to a possible southward located source vent. Note the general discrepancy between measured thicknesses and isopach maps. The measured thickness of layer B in brackets. The eruptions and the references are the same as in Fig. 11. All values are in cm.

a medial-proximal facies, and 20 cm at about 35 km from the source.

The Masaya Tuff isopach map (Fig. 11b) is in better agreement with the thickness values measured in the BFVA (especially in Sály), however Eger and Ostoros seems to be far from the characteristic distance-thickness rate of the Masaya Tuff at the same distance from the vent.

A "Hekla-scenario" (Fig. 11c) with easterly-directed wind fits pretty well to the thickness of layer B of the Mangó ignimbrite unit.

The isopach map of the Opepe Tephra (Fig. 11d) is in the best agreement with our results, however the 20 cm isopach line was observed a bit closer to the source than supposed for layer B. This tephra is also felsic, hence the physics of the pyroclast transport features is considered theoretically the most identical to the BFVA tephras.

If a southern source area is considered, the no-wind condition of the Pululagua eruption is applicable for the westernmost outcrops (Eger and Ostoros), but not for Szomolya and Sály (Fig. 12a). The Masaya Tuff isopach lines show more proximal and thicker facies for the fallout horizon for both outcrops (Fig. 12b). Isopach lines modified by a very directed and strong wind like that occurred during the 1104 CE eruption of Hekla volcano does not seem to be a realistic analogue for the layer B fallout layer (Fig. 12c), because it is not applicable for the Eger, Ostoros and Szomolya outcrops. The Taupo eruption (Opepe Tephra) with a southern source also does not fit for our measured thicknesses (Fig. 12d). Consequently, according to the fitting of our measured thicknesses of layer B to the isopach maps of well-known Plinian eruptions mentioned above, an eastern (north-eastern) source region seems to be more likely and more applicable than a southern one.

Conclusions

In this study three occurrences of a Lower Miocene fallout tephra in the Bükk Foreland Volcanic Area, Northern Hungary, were correlated via identical lithostratigraphic position, volcanological features such as field appearance and componentry, and identical paleomagnetic rotations, in order to determine the location of the source region.

This work is the first attempt to infer the spatial relationships of a particular unit (emplaced from a specific eruptive event) by applying quantitative thickness measurement and granulometrical analysis.

The three investigated outcrops (Eger – Tufakőbánya, Ostoros – Arany János street and Sály – Latorvár) were compared using magnetic-paleomagnetic and field volcanological properties. The upper (partially welded) ignimbrites at these outcrops were correlated by their primary paleomagnetic directions. Although primary paleomagnetic directions could not be isolated for the non-welded pyroclastic rocks, which are in lower stratigraphic position, they could also be correlated by their similar major magnetic-paleomagnetic properties.

The investigated sequence at the base of Mangó ignimbrite unit represents the opening phase of a Plinian event, which consists of a pyroclastic-fallout deposit, a deposit from a dilute PDC and an ignimbrite on the top. The average and maximum diameter of the lithic clasts separated from the pyroclastic-fallout deposit (layer B) apparently increases systematically toward the east. In addition, the thickness of the pyroclastic fallout also increases (Eger: 20 cm – Szomolya: 22 cm – Ostoros: 23 cm – Sály: 71 cm) eastward. Hence, the source region of the pyroclastic fallout layer of the Mangó ignimbrite unit and the associated ignimbrite and ground-surge deposit is inferred to be eastward (north-eastward) of the BFVA at a relatively close distance (~5–15 km from the easternmost site of Sály – Latorvár). Comparison between thickness data of this study and well-documented Plinian successions worldwide also supports a north-eastern source region. Moreover, the presence of welding in the ignimbrite only in the eastern locality, i.e. closest to the inferred source area, is also in agreement with the eastward origin.

The presented results imply, that if favourable outcrop patterns of ancient (e.g. Miocene) pyroclastic-fallout deposits are given, even in a relatively small number (i.e. three measurable sections), it is possible to locate the direction of the source region based on comparison with published isopach maps associated with Plinian fallout events.

Acknowledgements: This work was supported by the Hungarian Scientific Research Fund projects no. K115472, K128122, K128625 and K131894. Volcanological research of T.B. was supported by the ÚNKP-20-4 New National Excellence Program of the Ministry of Innovation and Technology from the source of the National Research, Development and Innovation Found (ÚNKP-20-4-II-ELTE-32). The research was supported by the European Union and the State of Hungary, co-financed by the European Regional Development Fund in the project GINOP-2.3.2.-15-2016-00009 'ICER'. We want to thank editor Lukáš Krmíček for handling of the manuscript, and Christoph Breitkreuz and Prokop Závada reviewers for the constructive and helpful comments.

References

Alfano F., Bonadonna C., Watt S., Connor C., Volentik A. & Pyle D.M. 2016: Reconstruction of total grain size distribution of the climactic phase of a long-lasting eruption: the example of the 2008–2013 Chaiten eruption. *Bulletin of Volcanology* 78, 46. https://doi.org/10.1007/s00445-016-1040-5

Arce J.L., Macías J.L. & Vázquez-Selem L. 2003: The 10.5 ka Plinian eruption of Nevado de Toluca volcano, Mexico: Stratigraphy and hazard implications. *Geological Society of America Bulletin* 115, 2, 230–348. https://doi.org/10.1130/0016-7606(2003)115<0230:tkpeon>2.0.co;2

Bice D.C. 1985: Quaternary volcanic stratigraphy of Managua, Nicaragua: Correlation and source assignment for multiple overlapping plinian deposits. *Geological Society of America Bulletin* 96, 553–566. https://doi.org/10.1130/0016-7606(1985)96<553:qvsomn>2.0.co;2

Biró T., Kovács I.J., Karátson D., Stalder R., Király E., Falus Gy., Fancsik T. & Kovács S.J. 2017: Evidence for post-depositional diffusional loss of hydrogen in quartz phenocryst fragments within ignimbrites. *American Mineralogist* 102, 1187–1201. https://doi.org/10.2138/am-2017-5861

Biró T., Hencz M., Németh K., Karátson D., Márton E., Szakács A., Bradák B., Szalai Z., Pécskay Z. & Kovács I.J. 2020: A Miocene Phreatoplinian eruption in the North-Eastern Pannonian Basin, Hungary: the Jató Member. *Journal of Volcanology and Geothermal Research* 401, 1–21. https://doi.org/10.1016/j.jvolgeores.2020.106973

Bonadonna C., Ernst G.G.J. & Sparks R.S.J. 1998: Thickness variations and volume estimates of tephra fall deposits: the importance of particle Reynolds number. *Journal of Volcanology and Geothermal Research* 81, 173–187. https://doi.org/10.1016/s0377-0273(98)00007-9

Branney M.J. & Kokelaar P. 1992: A reappraisal of ignimbrite emplacement: progressive aggradation and changes from particulate to non-particulate flow during emplacement of high-grade ignimbrite. *Bulletin of Volcanology* 54, 504–520. https://doi.org/10.1007/bf00301396

Buckland H.M., Cashman K.V., Engwell S.L. & Rust A.C. 2020: Sources of uncertainty in the Mazama isopachs and the implications for interpreting distal tephra deposits from large magnitude eruptions. *Bulletin of Volcanology* 82, 1–17. https://doi.org/10.1007/s00445-020-1362-1

Cagnoli B. & Tarling D.H. 1997: The reliability of anisotropy of magnetic susceptibility data as flow direction indicators in friable base surge and ignimbrite deposits: Italian examples. *Journal of Volcanology and Geothermal Research* 75, 309–320. https://doi.org/10.1016/s0377-0273(96)00038-8

Campbell M.E., Russel J.K. & Porritt L.A. 2013: Thermomechanical milling of accessory lithics in volcanic conduit. *Earth and Planetary Science Letters* 377–378, 276–286. https://doi.org/10.1016/j.epsl.2013.07.008

Capaccioni B., Coradossi N., Harangi R., Harangi Sz., Karátson D., Sarocchi D. & Valentini L. 1995: Early Miocene pyroclastic rocks of the Bükkalja Ignimbrite Field (North Hungary) – A preliminary stratigraphic report. *Acta Vulcanologica* 7, 119–124.

Coltelli M., Del Carlo P. & Vezzoli L. 2000: Stratigraphic constrains for explosive activity for the past 100 ka at Etna volcano, Italy. *International Journal of Earth Sciences* 89, 665–677. https://doi.org/10.1007/s005310000117

Csontos L., Nagymarosy A. & Horváth F. 1992: Tertiary evolution of the Intra-Carpathian area: A model. *Tectonophysics* 208, 221–241. https://doi.org/10.1016/b978-0-444-89912-5.50017-x

Druitt T.H. 1998: Pyroclastic density currents. In: Gilber J. & Sparks R.S.J. (Eds.): The Physics of Explosive Volcanic Eruptions. *Geological Society, London, Special Publications* 145, 145–182. https://doi.org/10.1144/gsl.sp.1996.145.01.08

Edgar C.J., Cas R.A.F., Olin P.H., Wolff J.A., Martí J. & Simmons J.M. 2017: Causes and complexity in a fallout dominated plinian eruption sequence: 312 ka Fasnia Member, Diego Hernández Formation, Tenerife, Spain. *Journal of Volcanology and Geothermal Research* 345, 21–45. https://doi.org/10.1016/j.jvolgeores.2017.07.008

Eychenne J., Le Pennec J.-L., Troncoso L., Gouhier M. & Nedelec J.-M. 2012: Causes and consequences of bimodal grain-size distribution of tephra fall deposited during the August 2006 Tungurahua eruption (Ecuador). *Bulletin of Volcanology* 74, 187–205. https://doi.org/10.1007/s00445-011-0517-5

Fierstein J. & Hildreth W. 1992: The plinian eruptions of 1912 at Novarupta, Katmai National Park, Alaska. *Bulletin of Volcanology* 54, 646–684. https://doi.org/10.1007/bf00430778

Fisher R.A. 1953: Dispersion on a sphere. *Proceedings of the Royal Society of London. Series A. Mathematical and Physical Sciences*, 217, 295–305. https://doi.org/10.1098/rspa.1953.0064

Fisher R.V. 1979: Models for pyroclastic surges and pyroclastic flows. *Journal of Volcanology and Geothermal Research* 6, 305–318. https://doi.org/10.1016/0377-0273(79)90008-8

Gubler T., Meier M. & Oberli F. 1992: Bentonites as Time Markers for Sedimentation of the Upper Freshwater Molasses: Geological Observations Corroborated by High Resolution Single Zircon U–Pb Ages. *SANV Annual Assembly*, Basel, 12–13.

Hámor G., Balogh K. & Ravasz-Baranyai L. 1978: The radiometric age of the Miocene rhyolite tuff horizons of Hungary. *Annual report of the Geological Institute of Hungary, 1978* 61–76 (in Hungarian).

Harangi Sz. & Lukács R. 2019: The Neogene to Quaternary volcanism and its geodynamic relations in the Carpathian–Pannonian Region. *Földtani Közlöny* 149, 197–232 (in Hungarian). https://doi.org/10.23928/foldt.kozl.2019.149.3.197

Harangi Sz., Mason P.R.D. & Lukács R. 2005: Correlation and petrogenesis of silicic pyroclastic rocks in the Northern Pannonian Basin, Eastern-Central Europe: In situ trace element data of glass shards and mineral chemical constraints. *Journal of Volcanology and Geothermal Research* 143, 237–257. https://doi.org/10.1016/j.jvolgeores.2004.11.012

Hildreth W. & Mahood G. 1985: Correlation of ash-flow tuffs. *Geological Society of America Bulletin* 96, 968–974. https://doi.org/10.1130/0016-7606(1985)96<968:COAT>2.0.CO;2

Houghton B.F., Carey R.J. & Rosenberg M.D. 2014: The 1800a Taupo eruption: „III wind" blows the ultraplinian type event down to plinian. *Geology* 42, 459–461. https://doi.org/10.1130/g35400.1

Janebo M.H., Thordarson T., Houghton B.F., Bonadonna C., Larsen G. & Carey R.J. 2016: Dispersal of key subplinian-Plinian tephras from Hekla volcano, Iceland: implications for eruption source parameters. *Bulletin of Volcanology* 78, 66. https://doi.org/10.1007/s00445-016-1059-7

Kirschvink J.L. 1980: The least-squares line and plane and the analysis of paleomagnetic data. *Geophysical Journal International* 62, 699–718. https://doi.org/10.1111/j.1365-246x.1980.tb02601.x

Kischer U., Mitchell R.N., Liu Y., Nordsvan A.R., Cox G.M., Pisarevsky S.A., Wang C., Wu L, Murphy J.B. & Li Z.-X. 2020: Paleomagnetic constraints on the duration of the Australia-Laurentia connection in the core of the Nuna supercontinent. *Geology*. https://doi.org/10.1130/G47823.1

Konečný V., Lexa J. & Hojstričová V. 1995: The Central Slovakian Volcanic Field: a review. *Acta Vulcanologica* 7, 63–78.

Kovács I. & Szabó Cs. 2008: Middle Miocene volcanism in the vicinity of the Middle Hungarian zone: Evidence for an inherited enriched mantle source. *Journal of Geodynamics* 45, 1–15. https://doi.org/10.1016/j.jog.2007.06.002

Kováč M., Andreyeva-Grigorovich A., Bajraktarevic Z., Brzobohatý R., Filipescu S., Fodor L., Harzhauser M., Nagymarosy A., Oszczypko N. & Pavelic D. 2007: Badenian evolution of the Central Paratethys Sea: Paleogeography, climate and eustatic sea-level changes. *Geologica Carpathica* 58, 579–606.

Kováč M., Hudáčková N., Halásová E., Kováčová M., Holcová K., Oszczypko-Clowes M., Báldi K., Less G., Nagymarosy A., Ruman A. & Klučiar T. 2017: The Central Paratethys palaeoceanography: a water circulation model based on microfossil proxies, climate, and changes of depositional environment. *Acta Geologica Slovaca* 9, 75–114.

Lexa J., Seghedi I., Németh K., Szakács A., Konečný V., Pécskay Z., Fülöp A. & Kovacs M. 2010: Neogene–Quaternary volcanic forms in the Carpathian–Pannonian Region: a review. *Central European Journal of Geosciences* 2, 207–270. https://doi.org/10.2478/v10085-010-0024-5

Lukács R., Harangi Sz., Ntaflos T. & Mason P.R.D. 2005: Silicate melt inclusions in the phenocrysts of the Szomolya Ignimbrite, Bükkalja Volcanic Field (Northern Hungary): Implications for magma chamber processes. *Chemical Geology* 223, 46–67. https://doi.org/10.1016/j.chemgeo.2005.03.013

Lukács R., Harangi Sz., Mason P.R. & Ntaflos T. 2009: Bimodal pumice populations in the 13.5 Ma Harsány ignimbrite, Bükkalja Volcanic Field, Northern Hungary: Syn-eruptive mingling of distinct rhyolitic magma batches? *Central European Geology* 52, 51–72. https://doi.org/10.1556/ceugeol.52.2009.1.4

Lukács R., Harangi Sz., Radóc Gy., Kádár M., Pécskay Z. & Ntaflos T. 2010: The Miocene pyroclastic rocks of the boreholes Miskolc–7, Miskolc–8 and Nyékládháza–1 and their correlation with the ignimbrites of Bükkalja. *Földtani Közlöny* 140, 31–48 (in Hungarian).

Lukács R., Harangi Sz., Bachmann O., Guillong M., Danišík M., Buret Y., von Quadt A., Dunkl I., Fodor L., Sliwinski J., Soós I. & Szepesi J. 2015: Zircon geochronology and geochemistry to constrain the youngest eruption events and magma evolution of the Mid-Miocene ignimbrite flare-up in the Pannonian Basin, eastern-central Europe. *Contributions to Mineralogy and Petrology* 170, 1–26. https://doi.org/10.1007/s00410-015-1206-8

Lukács R., Harangi Sz., Guillong M., Bachmann O., Fodor L., Buret Y., Dunkl I., Sliwinski J., von Quadt A., Peytcheva I. & Zimmerer M. 2018: Early to Mid-Miocene syn-extensional massive silicic volcanism in the Pannonian Basin (East-Central Europe): Eruption chronology, correlation potential and geodynamic implications. *Earth Science Reviews* 179, 1–19. https://doi.org/10.1016/j.earscirev.2018.02.005

Marti A., Folch A., Costa A. & Engwell S. 2016: Reconstructing the plinian and co-ignimbrite sources of large volcanic eruptions: A novel approach for the Campanian Ignimbrite. *Scientific Reports* 6, 21220. https://doi.org/10.1038/srep21220

Martí J., Groppelli G. & Brum de Silveira A. 2018: Volcanic stratigraphy: A review. *Journal of Volcanology and Geothermal Research* 357, 68–91. https://doi.org/10.1016/j.jvolgeores.2018.04.006

Márton E. & Márton P. 1996: Large scale rotations in North Hungary during the Neogene as indicated by paleomagnetic data. In: Morris A. & Tarling D.H. (Eds.): Paleomagnetism and Tectonics of the Mediterranean Region. *Geological Society Special Publication* 105, 153–173. https://doi.org/10.1144/gsl.sp.1996.105.01.15

Márton E. & Pécskay Z. 1998: Complex evaluation of paleomagnetic and K/Ar isotope data of the Miocene ignimbritic volcanics in the Bükk Foreland, Hungary. *Acta Geologica Hungarica* 41, 467–476.

Márton E., Márton P. & Zelenka T. 2007: Paleomagnetic correlation of Miocene pyroclastics of the Bükk Mts and their forelands. *Central European Geology* 50, 47–57. https://doi.org/10.1556/ceugeol.50.2007.1.4

McFadden P.L. & McElhinny M.W. 1988: The combined analysis of remagnetization circles and direct observations in paleomagnetism. *Earth and Planetary Science Letters* 87, 161–172. https://doi.org/10.1016/0012-821x(88)90072-6

Mele D., Costa A., Dellino P., Sulpizio R., Dioguardi F., Isaia R. & Macedonio G. 2020: Total grain size distribution of components of fallout deposits and implications for magma fragmentation mechanism: examples from Campi Flegrei caldera (Italy).

Bulletin of Volcanology 82, 1–12. https://doi.org/10.1007/s00445-020-1368-8

Mothes P.A. & Hall M. L. 2008: The plinian fallout associated with Quilotoa's 800 yr BP eruption, Ecuadorian Andes. *Journal of Volcanology and Geothermal Research* 176, 56–69. https://doi.org/10.1016/j.jvolgeores.2008.05.018

Németh K. & Palmer J. 2019: Geological mapping of volcanic terrains: Discussion on concepts, facies models, scales, and resolutions from New Zealand perspective. *Journal of Volcanology and Geothermal Research* 385, 27–45. https://doi.org/10.1016/j.jvolgeores.2018.11.028

Noszky J. 1931: The Oligocene–Miocene stratigraphy of the northeastern part of the Hungarian Mid-Mountains: II. The Miocene. *Annual report of the Geological Institute of Hungary* 27, 160–236 (in Hungarian).

Ort M.H., Newkirk T.T., Vilas J.F. & Vazquez J.A. 2015: Towards the definition of AMS facies in the deposits of pyroclastic density currents. In: Ort M.H., Porreca M. & Geissman J.W. (Eds.): The Use of Paleomagnetism and Rock Magnetism to Understand Volcanic Processes. *Geological Society, London, Special Publications* 396, 205–226. https://doi.org/10.1144/sp396.8

Pantó G. 1961: Evolution of the ignimbrit issue and its Hungarian dimension. *MTA Műszaki Tudományok Osztálya Közleményei* 29, 299–322 (in Hungarian).

Pantó G. 1962: The role of ignimbrites in the volcanism of Hungary. *Acta Geologica Hungarica* 6, 307–331.

Papale P. & Rosi M. 1993: A case of no-wind plinian fallout at Pululagua caldera (Ecuador): implications for models of clast dispersal. *Bulletin of Volcanology* 55, 523–535. https://doi.org/10.1007/bf00304594

Pécskay Z., Lexa J., Szakács A., Seghedi I., Balogh K., Konečný V., Zelenka T., Kovács M., Póka T., Fülöp A., Márton E., Panaiotu C. & Cvetković V. 2006: Geochronology of Neogene magmatism in the Carpathian arc and intra-Carpathian area. *Geologica Carpathica* 57, 511–530.

Pedrazzi D., Sunye-Puchol I., Aguirre-Díaz G., Costa A., Smith V.C., Poret M., Dávila-Harris P., Miggins D.P., Hernández W. & Gutiérrez E. 2019: The Ilopango Tierra Blanca Joven (TBJ) eruption, El Salvador: Volcano-stratigraphy and physical characterization of the major Holocene event of Central-America. *Journal of Volcanology and Geothermal Research* 377, 81–102. https://doi.org/10.1016/j.jvolgeores.2019.03.006

Pioli L. & Rosi M. 2005: Rheomorphic structures in a high-grade ignimbrite: The Nuraxi tuff, Sulcis volcanic district (SW Sardinia, Italy). *Journal of Volcanology and Geothermal Research* 142, 11–28. https://doi.org/10.1016/j.jvolgeores.2004.10.011

Póka T. Zelenka T., Szakács A., Seghedi I., Nagy G. & Simonits A. 1998: Petrology and geochemistry of the Miocene acidic explosive volcanism of the Bükk Foreland; Pannonian Basin, Hungary. *Acta Geologica Hungarica* 41, 399–428.

Pyle D.M., Ricketts G.D., Margari V., van Andela T.H., Sinitsyn A.A., Praslov N.D. & Lisitsyn S. 2006: Wide dispersal and deposition of distal tephra during the Pleistocene 'Campanian Ignimbrite/Y5' eruption, Italy. *Quaternary Science Reviews* 25, 2713–2728. https://doi.org/10.1016/j.quascirev.2006.06.008

Randolph-Flagg N., Breen S., Hernandez A., Manga M. & Self S. 2017: Evenly spaced columns in the Bishop Tuff (California) as relicts of hydro-thermal cooling. *Geology* 45, 1015–1018. https://doi.org/10.1130/g39256.1

Rocholl A., Schaltegger U., Gilg H.A., Wijbrans J. & Böhme M. 2017: The age of volcanic tuffs from the Upper Freshwater Molasse (North Alpine Foreland Basin) and their possible use for tephrostratigraphic correlations across Europe for the Middle Miocene. *International Journal of Earth Sciences* 107, 387–407. https://doi.org/10.1007/ s00531-017-1499-0

Rybár S., Šarinová K., Sant K., Kuiper K.F., Kováčová M.,Vojtko R., Reiser M.K., Fordinál K., Teodoridis V., Nováková P. & Vlček T. 2019: New $^{40}Ar/^{39}Ar$, fission track and sedimentological data on a middle Miocene tuff occurring in the Vienna Basin: Implications for the north-western Central Paratethys region. *Geologica Carpathica* 70, 386–404. https://doi.org/10.2478/geoca-2019-0022

Schréter Z. 1939: Geological properties of the southeastern side of the Bükk Mountains. *Annual report of the Geological Institute of Hungary 1933-35*, 511–532 (in Hungarian).

Seghedi I., Downes H., Szakács A., Mason P.R.D., Thirlwall M.F., Rosu E., Pécskay Z., Márton E. & Panaiotu C. 2004: Neogene–Quaternary magmatism and geodynamics in the Carpathian–Pannonian region: a synthesis. *Lithos* 72, 117–146. https://doi.org/10.1016/j.lithos.2003.08.006

Seghedi I., Downes H., Harangi Sz., Mason P. R. & Pécskay Z. 2005: Geochemical response of magmas to Neogene–Quaternary continental collision in the Carpathian–Pannonian region: a review. *Tectonophysics* 410, 485–499. https://doi.org/10.1016/j.tecto.2004.09.015

Simmons J.M., Cas R.A.F., Druitt T.H. & Carey R.J. 2017: The initiation and development of a caldera-forming Plinian eruption (172 ka Lower Pumice 2 eruption, Santorini, Greece). *Journal of Volcanology and Geothermal Research* 341, 332–350. https://doi.org/10.1016/j.jvolgeores.2017.05.034

Solleiro-Rebolledo E., Sedov S., Gama-Castro J., Flores-Román D. & Ecamilla-Sarabia G. 2003: Paleosol-sedimentary sequences of the Glacis de Buenavista, Central Mexico: interaction of Late Quaternary pedogenesis and volcanic sedimentation. *Quaternary International* 106–107, 185–201. https://doi.org/10.1016/s1040-6182(02)00172-6

Sparks R.S.J., Self S. & Walker G.P. 1973: Products of ignimbrite eruptions. *Geology* 1, 115–118. https://doi.org/10.1130/0091-7613(1973)1%3C115:poie%3E2.0.co;2

Sparks R.S.J., Bursik M.I., Ablay G.J., Thomas R.M.E. & Carey S.N. 1992: Sedimentation of tephra by volcanic plumes. Part 2: controls on thickness and grain-size variations of tephra fall deposits. *Bulletin of Volcanology* 54, 685–695. https://doi.org/10.1007/bf00430779

Sparks R.S.J., Gardeweg M.C., Calder E.S. & Matthews S.J. 1997: Erosion by pyroclastic flows on Lascar Volcano, Chile. *Bulletin of Volcanology* 58, 557–565. https://doi.org/10.1007/s004450050162

Streck M.J. & Grunder A.L. 1995: Crystallization and welding variations in a widespread ignimbrite sheet; the Rattlesnake Tuff, eastern Oregon, USA. *Bulletin of Volcanology* 57, 151–169. https://doi.org/10.1007/s004450050086

Szabó Cs., Harangi Sz. & Csontos L. 1992: Review of Neogene and Quaternary volcanism of the Carpathian-Pannonian Region. *Tectonophysics* 208, 243–256. https://doi.org/10.1016/0040-1951(92)90347-9

Szakács A. & Karátson D. 1997: The Inner-Carpathian calc-alkaline volcanism. Plate tectonic interpretation of the Carpatho–Pannonian Region. In: Karátson D. (Ed.): Pannon Enciklopédia – Magyarország földje. Budapest, 73–77 (in Hungarian).

Szakács A., Márton E., Póka T., Zelenka T., Pécskay Z. & Seghedi I. 1998: Miocene acidic explosive volcanism in the Bükk Foreland, Hungary: Identifying eruptive sequences and searching for source locations. *Acta Geologica Hungarica* 41, 413–435.

Szakács A., Pécskay Z., Silye L., Balogh K., Vlad D. & Fülöp A. 2012: On the age of the Dej Tuff, Transylvanian Basin (Romania). *Geologica Carpathica* 63, 139–148. https://doi.org/10.2478/v10096-012-0011-9

Szakács A., Pécskay Z. & Gál Á. 2018: Patterns and trends of time–space evolution of Neogene volcanism in the Carpathian–Pannonian region: a review. *Acta Geodaetica et Geophysica* 53, 347–367. https://doi.org/10.1007/s40328-018-0230-3

Valentine G.A. 2020: Initiation of dilute and concentrated pyroclastic currents from collapsing mixtures and origin of their proximal deposits. *Bulletin of Volcanology* 82, 1–24. https://doi.org/10.1007/s00445-020-1366-x

Vespa M., Keller J. & Gertisser R. 2006: Interplinian explosive activity of Santorini volcano (Greece) during the past 150,000 years. *Journal of Volcanology and Geothermal Research* 153, 262–286. https://doi.org/10.1016/j.jvolgeores.2005.12.009

Walker G.P.L. 1971: Grain-size characteristics of pyroclastic deposits. *Journal of Volcanology and Geothermal Research* 79, 696–714. https://doi.org/10.1086/627699

Walker G.P.L. 1980: The Taupo pumice: Product of the most powerful known (ultraplinian) eruption? *Journal of Volcanology and Geothermal Research* 8, 69–94. https://doi.org/10.1016/0377-0273(80)90008-6

Walker G.P.L. 1983: Ignimbrite types and ignimbrite problems. *Journal of Volcanology and Geothermal Research* 17, 65–88. https://doi.org/10.1016/0377-0273(83)90062-8

Wilson C.J.N. 1993: Stratigraphy, chronology, styles and dynamics of late Quaternary eruptions from Taupo volcano, New Zealand. *Philosophical Transactions: Physical Sciences and Engineering*, 343, 205–306. https://doi.org/10.1098/rsta.1993.0050

Wilson C.J.N. 2001: The 26.5 ka Oruanui eruption, New Zealand: an introduction and overview. *Journal of Volcanology and Geothermal Research* 112, 133–174. https://doi.org/10.1016/s0377-0273(01)00239-6

Wotzlaw J.-F., Hüsing S.K., Hilgen F.J. & Schaltegger U. 2014: High-precision zircon U-Pb geochronology of astronomically dated volcanic ash beds from the Mediterranean Miocene. *Earth and Planetary Science Letters* 407, 19–34. https://doi.org/10.1016/j.epsl.2014.09.025

Wright J.V. & Walker G.P.L. 1981: Eruption, transport and deposition of ignimbrite: a case study from Mexico. *Journal of Volcanology and Geothermal Research* 9, 111–131. https://doi.org/10.1016/0377-0273(81)90001-9

Electronic supplementary material is available online:

Supplement S1 "Satellite image of Eger – Tufakőbánya site" at http://geologicacarpathica.com/data/files/supplements/Hencz_Supplement1.jpg.

Supplement S2 "Satellite image of Ostoros – Arany János street site" at http://geologicacarpathica.com/data/files/supplements/Hencz_Supplement2.jpg.

Supplement S3 "Satellite image of Sály – Latorvár site" at http://geologicacarpathica.com/data/files/supplements/Hencz_Supplement3.jpg.